

## Distinct mechanisms of B and T lymphocyte accumulation generate tumor-draining lymph node hypertrophy

Lauren M. Habenicht<sup>a</sup>, Tina C. Albershardt<sup>b</sup>, Brian M. Iritani<sup>a</sup>, and Alanna Ruddell<sup>a,b</sup>

<sup>a</sup>Department of Comparative Medicine, University of Washington, Seattle, WA, USA; <sup>b</sup>Fred Hutchinson Cancer Research Center, Seattle, WA, USA

### ABSTRACT

Tumor-draining lymph nodes (TDLNs) often enlarge in human cancer patients and in murine tumor models, due to lymphocyte accumulation and lymphatic sinus growth. B lymphocytes within TDLNs can drive lymph node hypertrophy in response to tumor growth, however little is known about the mechanisms directing the preferential accumulation of B lymphocytes relative to T cells in enlarging TDLNs. To define why B and T lymphocytes accumulate in TDLNs, we quantified lymphocyte proliferation, apoptosis, entry, and exit in TDLNs versus contralateral non-TDLNs (NTDLNs) in a footpad B16-F10 melanoma mouse model. B and T lymphocyte proliferation and apoptosis were increased as the TDLNs enlarged, although relative rates were similar to those of NTDLNs. TDLN entry of B and T lymphocytes via high endothelial venules was also modestly increased in enlarged TDLNs. Strikingly, the egress of B cells was strongly reduced in TDLNs versus NTDLNs, while T cell egress was modestly decreased, indicating that regulation of lymphocyte exit from TDLNs is a major mechanism of preferential B lymphocyte accumulation. Surface sphingosine-1-phosphate receptor 1 (S1PR1) which binds S1P and signals lymphocyte egress, exhibited greater downregulation in B relative to T lymphocytes, consistent with preferential retention of B lymphocytes in TDLNs. TDLN lymphocytes did not activate surface CD69 expression, indicating a CD69-independent mechanism of downregulation of S1PR1. B and T cell trafficking via afferent lymphatics to enter TDLNs also increased, suggesting a pathway for accumulation of tumor-educated lymphocytes in TDLNs. These mechanisms regulating TDLN hypertrophy could provide new targets to manipulate lymphocyte responses to cancer.

### ARTICLE HISTORY

Received 16 March 2016  
Revised 15 June 2016  
Accepted 17 June 2016

### KEYWORDS

Afferent lymph; chemokines; lymphocyte activation; lymph node; lymphocyte trafficking; lymphatic sinuses; melanoma; sphingosine-1-phosphate receptor 1

### Introduction

Tumor-draining lymph nodes (TDLNs) often enlarge in human cancer patients<sup>1,2</sup> and murine tumor models.<sup>3-5</sup> Enlarged TDLNs can demonstrate extensive remodeling, featuring disproportionate accumulation of B lymphocytes<sup>3,6,7</sup> and extensive lymphatic sinus growth (lymphangiogenesis).<sup>2,4,8</sup> Lymphangiogenesis in TDLNs has been correlated with poor prognosis in patients with breast, rectal, and skin cancers.<sup>9-11</sup> Similarly, B cell accumulation and lymphangiogenesis characterize TDLNs in murine melanoma, squamous cell carcinoma, and lymphoma models.<sup>3,5,8</sup> Repetition in these findings across species and tumor types demonstrates the translational relevance of determining the underlying mechanism of TDLN hypertrophy, to understand how accumulation of lymphocytes in TDLNs could contribute to the antitumor immune response.

A syngeneic, immunocompetent mouse model of a solid tumor (melanoma) was selected to study the mechanisms of TDLN hypertrophy. The B16-F10 footpad melanoma model in C57BL/6 mice is ideal for studying TDLN responses to tumor growth, because in the first 3 weeks slow growth of these tumors induces a local rather than systemic immune response to the tumor, enabling direct comparison of the TDLN to the contralateral non-tumor draining popliteal lymph node (NTDLN) within the same mouse.<sup>12</sup> In this model, TDLNs feature an 8-fold increase in B cells and a 3-

fold increase in T cells, which creates a B-cell predominant environment within TDLNs.<sup>3</sup> The B cells in TDLNs are necessary for inducing extensive lymphangiogenesis and an accompanying 20-fold increase in TDLN lymph flow. Relative to a normal, or NTDLN, the architecture of TDLNs is strikingly altered, with growth of cortical and medullary sinuses and expansion of B cells deep into the paracortical areas normally occupied by T cells. These changes are associated with an ineffective antitumor immune response, which allows tumor growth and strongly promotes metastasis.<sup>12,13</sup>

Despite the importance of TDLN lymphocytes in cancer progression, the mechanisms of lymphocyte accumulation in TDLNs are poorly understood. Draining lymph node (LN) hypertrophy is also characteristic of a local response to inflammation or infection, and similar mechanisms could contribute to TDLN hypertrophy, though this has not been examined previously. LN lymphocytes are exposed to foreign and self-antigens displayed by antigen-presenting cells (APCs) in lymph fluid to direct the early immune response. During inflammation, B cell-driven lymphangiogenesis further promotes recruitment of dendritic cells from an inflamed area to the draining lymph node, which primes an expanding population of specialized high endothelial venules (HEVs) to promote adhesion and migration of lymphocytes into draining LNs.<sup>14-16</sup> Cellular

accumulation in draining LNs is enhanced by an acute, transient decrease in lymphocyte exit, facilitated by decreased signaling through the sphingolipid receptor S1PR1 on activated lymphocytes.<sup>17</sup> Stimulated lymphocytes in the draining LNs proliferate, resulting in expansion of specific effector cell populations.<sup>18,19</sup> Together, these draining LN changes promote an effective adaptive immune response against infectious agents.

In contrast to acute inflammation models, TDLN hypertrophy appears to be associated with a suppressed immune response,<sup>20,21</sup> implying key differences in these forms of cellular accumulation within the LN. For example, B16-F10 melanoma cells are rapidly eliminated when implanted into NTDLNs, but survive and expand when implanted within TDLNs.<sup>21</sup> The mechanisms underlying tumor-driven LN immune-suppression are poorly understood, but could be related to the architectural and compositional changes observed in TDLNs, including preferential B cell accumulation and extensive lymphatic sinus growth. Recently, a subset of regulatory B cells enriched in TDLNs has been identified which promotes B16-F10 melanoma tumor growth.<sup>12</sup> Additionally, LN lymphatic endothelial cells can induce lymphocyte anergy and activation-induced cell death (AICD), a form of apoptosis, by presenting antigens without providing co-stimulation.<sup>22,23</sup> Therefore, the B cell-dependent growth of TDLN lymphatic sinuses could play an important role in suppression of the antitumor immune response.

In this study, we used the B16-F10 footpad melanoma model to investigate local and rapid increases in TDLN size and lymphocyte cellularity. Lymphocyte proliferation, apoptosis, entry, and exit were compared between NTDLNs and TDLNs. Additionally, chemokine receptors and other cell surface markers were compared between lymphocyte populations, to better characterize the differences which could distinguish B and T cell accumulation in TDLNs. Understanding the mechanisms of TDLN hypertrophy including preferential B cell accumulation could suggest new strategies for reversing or preventing tumor tolerance, to improve tumor immunotherapy.

## Results

After 3 weeks of B16-F10 tumor growth in a footpad, TDLNs are larger than NTDLNs, with increased numbers of lymphocytes and marked architectural changes that could affect the antitumor immune response. At this early time point, metastasis to TDLNs was rare, occurring in less than 10% of TDLNs ( $n = 62$ ). TDLNs demonstrated a 6-fold increase in lymphocyte cellularity compared to NTDLNs (Figs. 1A and B), with preferential accumulation of B cells compared to non-B cells (Fig. 1C). Lymphocytes identified as negative for B cell markers on flow cytometry are predominantly T cells (93% CD3e, CD4<sup>+</sup>, and/or CD8<sup>+</sup>) in mouse popliteal lymph nodes, and are termed “non-B cells” ( $n = 24$  popliteal LNs from 12 mice). B lymphocytes were largely confined to cortical follicles, while T cells occupied the central paracortex and medulla of NTDLNs (Fig. 1D). In TDLNs, B cells spread into the central paracortex and toward the medulla, while most T cells retained paracortical localization. Lymphatic sinuses were limited to the medulla and subcapsular regions of NTDLNs, while in TDLNs the lymphatic sinuses consistently grew<sup>3</sup> and extended into the paracortical and follicular regions of TDLNs (Fig. 1E). These comparisons demonstrate that the relationships of B and T

lymphocytes with the lymphatic sinuses (and likely other stromal components) are profoundly rearranged in TDLNs, which could influence their trafficking and immune functions.

### **Lymphocyte proliferation and apoptosis are proportional to TDLN size**

The overall increase in the TDLN lymphocyte population and preferential accumulation of B lymphocytes in LNs draining B16-F10 footpad tumors<sup>3</sup> suggests that the mechanisms regulating TDLN lymphocyte accumulation differ between B and T cells. Both types of lymphocytes are exposed to tumor antigen from the lymph in TDLNs, presented by APCs, which could activate the cells and induce proliferation.<sup>24,25</sup> Increased cellularity and preferential B cell accumulation in TDLNs could therefore result from increased cellular proliferation. To assess B and T cell proliferation, the incorporation of BrdU into dividing B and non-B lymphocytes was assessed by flow cytometry and compared in TDLNs and contralateral NTDLNs (Fig. 2A). The total number of proliferating B cells was not significantly increased in TDLNs relative to NTDLNs, although a trend was apparent (Fig. 2B). In contrast, TDLNs display a 12-fold increase in non-B cell proliferation by absolute numbers (Fig. 2C). Due to the increased cellularity of TDLNs,<sup>3</sup> the number of proliferating lymphocytes was also analyzed as a percent of the B and non-B cell populations within the LNs. By this measure, the percent proliferating B and T lymphocytes was similar in TDLNs versus NTDLNs (Figs. 2D and E). This data demonstrates that the increase in total numbers of proliferating B and T lymphocytes (especially T cells) contribute to TDLN hypertrophy, however other mechanisms must account for preferential B cell accumulation in TDLNs.

If the relative amount of proliferating lymphocytes in TDLNs is unchanged relative to NTDLNs, perhaps changes in rates of apoptosis could account for the observed hyper-cellularity and B cell enrichment in TDLNs. To determine whether TDLN hyper-cellularity and B lymphocyte enrichment could be caused by reductions in apoptosis, cleaved (active) caspase-3 was quantified in TDLN and contralateral NTDLN lymphocytes using flow cytometry (Fig. 3A). Contrary to our hypothesis, we observed a trend toward increased numbers of apoptotic B cells in TDLNs (Fig. 3B). In addition, the total number of apoptotic non-B cells (Fig. 3C), including both CD4<sup>+</sup> (Fig. 3D) and CD8<sup>+</sup> (Fig. 3E) T cell populations were increased within TDLNs. The overall percentage of apoptotic B and T cells were unchanged in TDLNs relative to NTDLNs (Figs. 3F–I), indicating that a reduced rate of lymphocyte apoptosis does not account for lymphocyte accumulation in TDLNs.

### **Increased lymphocyte entry into TDLNs partially accounts for cellular accumulation**

Increased lymphocyte entry via HEVs is thought to be a major mechanism regulating lymph node hypertrophy in inflammation.<sup>14,26</sup> To determine whether increased lymphocyte entry drives their accumulation in TDLNs, we transferred CFSE-labeled splenocytes from syngeneic, age-matched donor littermates into footpad B16-F10 melanoma-bearing mice, and quantified the number of labeled cells recovered

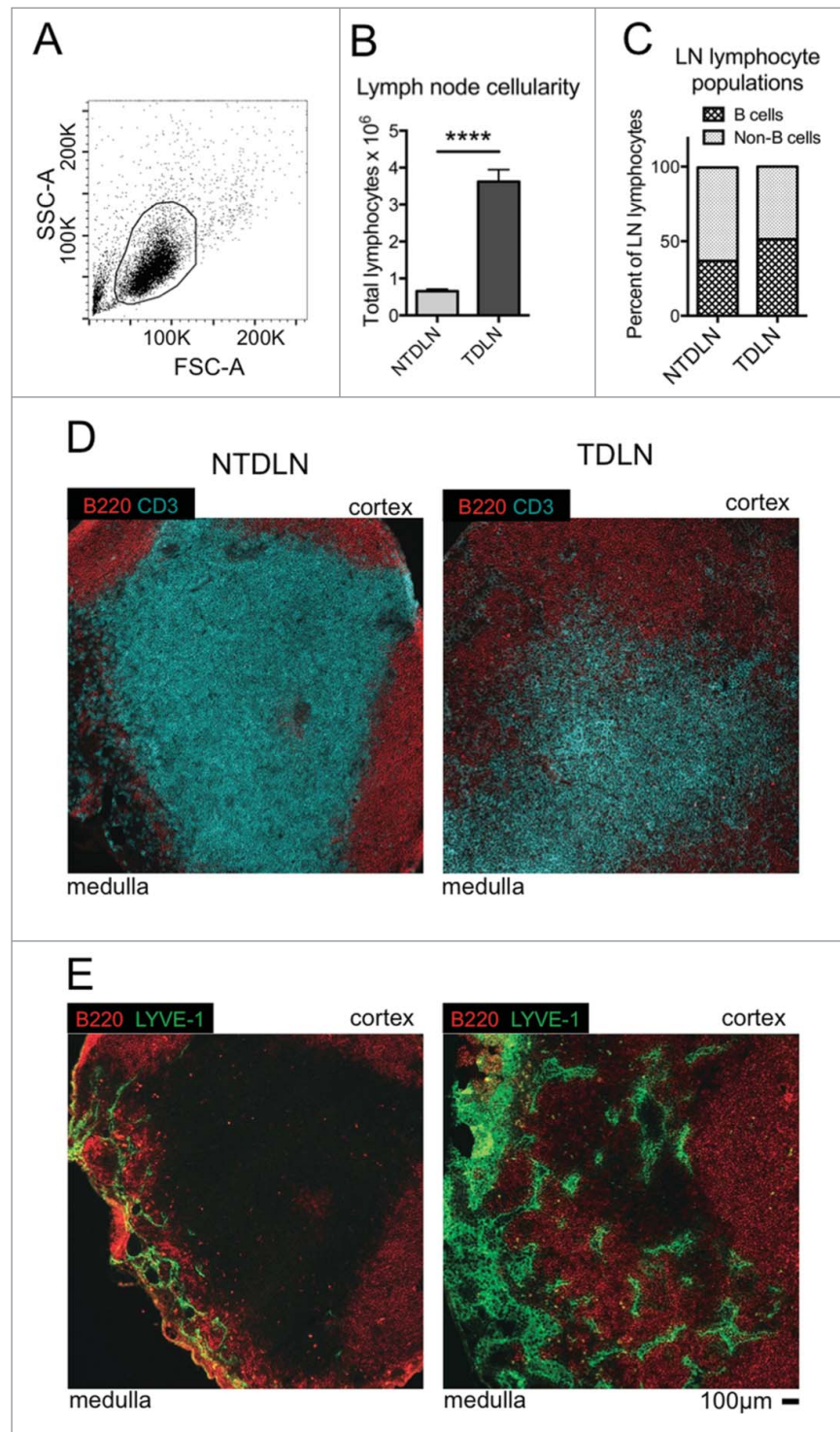


**Figure 1.** TDLNs demonstrate increased cellularity, preferential B cell accumulation, and architectural changes compared to NTDLNs. (A) Representative dot plot of forward and side scatter profiles for a C57BL/6 popliteal lymph node with gating strategy to identify lymphocytes. (B) Total lymphocyte cellularity of NTDLNs and TDLNs ( $n = 62$  paired LNs,  $p < 0.0001$ ). (C) Percentage of B and non-B cell lymphocyte populations in NTDLNs and TDLNs, determined by B220 staining on flow cytometry ( $n = 62$ ). (D) Immunofluorescent histology of representative NTDLNs and TDLNs, depicting infiltration of B cells (B220-positive, red) into T cell zone (CD3-positive, cyan) in TDLNs. (E) Lymphatic sinuses (LYVE-1-positive, green) expand in the medulla and central paracortex in TDLNs compared to NTDLNs. Cortical and medullary or paracortical regions of each LN are labeled to facilitate comparison of NTDLNs and TDLNs. Scale bar = 100  $\mu$ m for all images in (D) and (E).

from TDLNs and NTDLNs 2 h post-transfer (Fig. 4A). The 2 h time point was selected to ensure that lymphocytes had sufficient time to enter the popliteal LN in detectable numbers, but not enough time to traverse the LN and exit.<sup>27,28</sup> Two hours after intravenous transfer, labeled lymphocytes

were detectable in both NTDLNs and TDLNs (Fig. 4B). Labeled B and non-B lymphocytes were both much more numerous in TDLNs compared to NTDLNs (Figs. 4C and D), demonstrating that increased entry of lymphocytes contributes to TDLN hypertrophy.

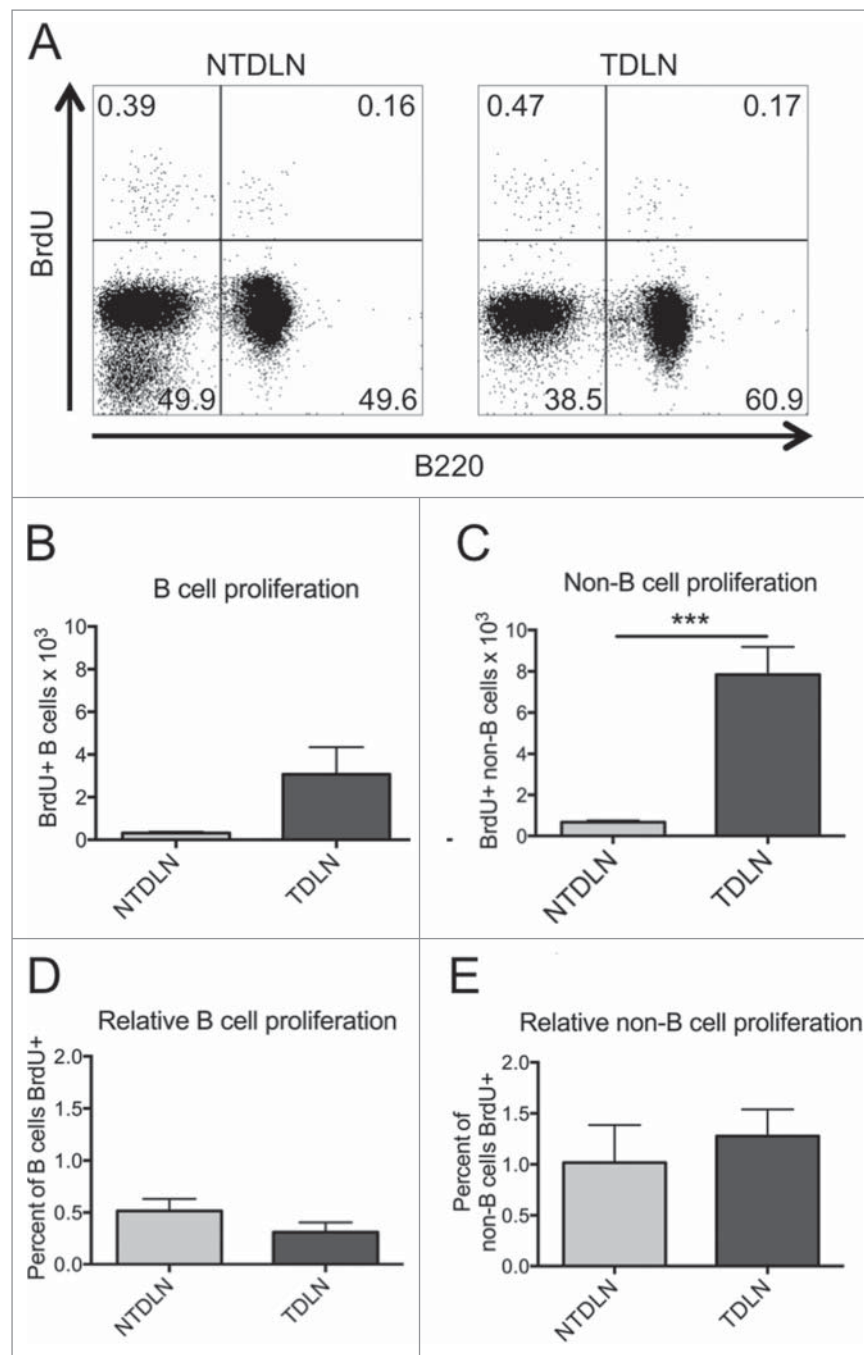


**Figure 2.** Increased lymphocyte proliferation in TDLNs is proportional to lymphocyte number. (A) Representative dot plot of proliferating lymph node lymphocytes as demonstrated by BrdU incorporation. (B) Total numbers of BrdU-positive B lymphocytes in mouse NTDLNs and TDLNs demonstrate a trend toward increased B cell proliferation in TDLNs ( $p = 0.07$ ). (C) An increased population of proliferative non-B cells is present in TDLNs compared to NTDLNs ( $p = 0.0008$ ). Overall, B lymphocyte (D) and non-B lymphocyte proliferation (E) is proportional to these populations in TDLNs ( $p = 0.13, p = 0.85$ , respectively). ( $n = 8$  paired LNs in three independent experiments, mean + SEM depicted).

To determine if increased entry of B cells relative to T cells could account for the preferential accumulation of B cells in TDLNs, we compared the ratio of labeled B and non-B cells in TDLNs to NTDLNs. On average, six B cells entered TDLNs for every B cell that entered NTDLNs during the 2 h equilibration time (Fig. 4E). Comparatively, an average of three non-B cells entered TDLNs for every non-B cell that entered NTDLNs. However, pairwise comparison of the ratio of B and T cell entry in each mouse revealed no significant difference in TDLN lymphocyte entry behavior (Fig. 4E). These findings suggest that while a higher rate of both B and T lymphocyte entry

contributes to TDLN hypertrophy it does not account for the preferential accumulation of B cells in TDLNs.

### **B cells are preferentially retained in TDLNs**

A decrease in the egress of lymphocytes from TDLNs via efferent lymphatics could also potentially contribute to hypercellularity and preferential B cell accumulation. A modified labeled-lymphocyte experiment was used to test whether reduced lymphocyte exit from TDLNs could



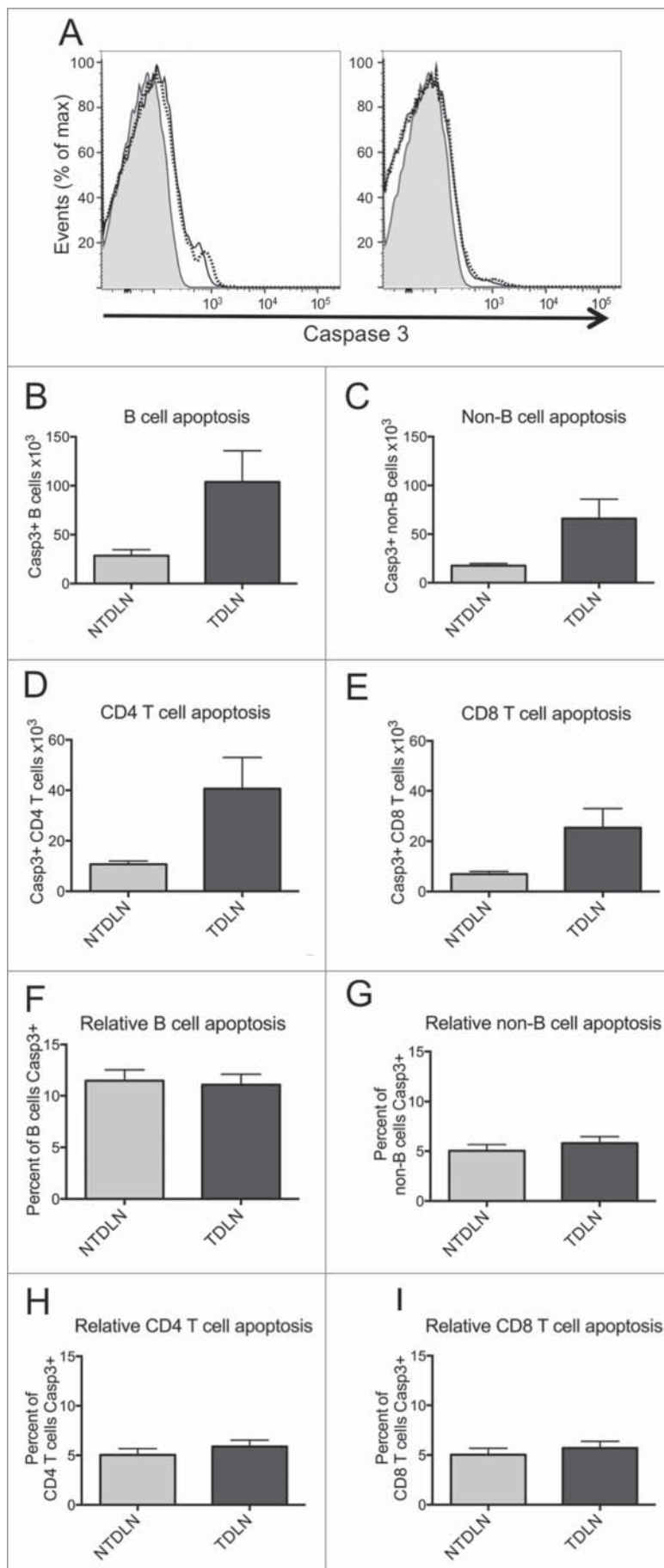


Figure 3. (For figure legend, see page 6.)

account for this phenotype. Circulating B cells enter and exit the lymph node with a half-life of over 24 h; T cells move through the lymph node more rapidly, with a half-life of 6–12 h.<sup>29</sup> To capture the kinetics of both B and non-B cells, we evaluated the number of labeled lymphocytes retained within TDLNs and NTDLNs by flow cytometry 20 h after IV transfer (Figs. 5A and B). Pairwise comparison of labeled lymphocytes in the TDLN and contralateral NTDLN of each mouse enabled simultaneous comparison of B and non-B cell retention. Strikingly, the populations of labeled B cells (Fig. 5C) and non-B cells (Fig. 5D) were significantly larger in TDLNs than NTDLNs. Compared to NTDLNs, there was an 11-fold increase in labeled B cells in TDLNs, and a 5-fold increase in labeled non-B cells (Fig. 5E). These findings suggest that the preferential accumulation of B cells in TDLNs involves increased retention of these cells within the TDLN.

These observations could also potentially be explained by a selective increase in labeled B cells continuing to enter TDLNs relative to T cells. To isolate rapid lymphocyte entry and track the egress of these cells from NTDLNs and TDLNs, mice were dosed systemically with an anti-L-selectin (CD62L) blocking antibody 2 h after labeled-lymphocyte transfer. Lymphocyte interaction with CD62L expressed on HEV endothelial cells is required for lymphocyte diapedesis and entry into LNs from the blood.<sup>30</sup> Quantification of labeled B and T cells 24 h later assessed the fate of cells that entered TDLNs and NTDLNs from the blood within the 2 h equilibration window (Fig. 6A). The 24 h time point was chosen to focus on the kinetics of B cells exiting TDLNs and NTDLNs. As expected, anti-CD62L treatment resulted in decreased NTDLN and TDLN cellularity compared to previous experiments, which confirmed the efficacy of the L-selectin antibody dose.<sup>31</sup> Relative to the experiment described in Fig. 4, total numbers of labeled B and T lymphocytes in TDLNs were significantly lower after entry blockade by anti-L-selectin (Figs. 6B and C). 9-fold more labeled B cells were recovered from TDLNs after entry arrest, as well as 12-fold more non-B cells (Fig. 6D). B cell egress behavior was similar with or without entry blockade (refer to Fig. 5E for comparison), indicating that selective reduction of B cell egress is a major mechanism of preferential B cell accumulation in TDLNs.

### Enhanced lymphocyte entry into TDLNs via afferent lymphatics

Surprisingly, after blockade of entry into HEVs, the TDLN:NTDLN ratio for non-B cells was increased (Fig. 6D). Following a 2 h entry window and an additional 24 h to exit the LNs, we expected to find very few labeled non-B cells in NTDLNs and TDLNs due to their rapid entry and exit kinetics. Instead, the non-B cell population was enriched in TDLNs compared to NTDLNs after entry arrest, two times more than we had observed during the

first exit experiment, 20 h after IV administration of labeled cells (Figs. 5E and 6D). This finding suggests an alternate mode of ongoing T cell entry into TDLNs that is not regulated by L-selectin.

The ability of naive lymphocytes to enter the lymph node via the afferent lymphatics is thought to be limited (reviewed in ref. <sup>36</sup>), due in part to very small numbers of lymphocytes within the afferent lymph.<sup>32</sup> Under normal conditions, naive T cell trafficking through non-lymphoid tissue, such as liver, can occur over one or more days.<sup>33</sup> To assess the entry of lymphocytes into TDLNs and NTDLNs via afferent lymph, splenocytes from naive, syngeneic donor mice were labeled with CFSE or CellTrace Violet (CTV). Cells with one of these fluorescent labels were injected into the dorsal subcutaneous space of the B16-F10 tumor-bearing foot (CFSE cells) and the contralateral non-tumor-bearing foot (CTV cells) of mice after 3 weeks of tumor growth (Fig. 7A). Lymph drains from this area to the corresponding ipsilateral and contralateral popliteal lymph nodes, respectively.<sup>34</sup> Twenty-four hours later, movement of the labeled cells into the draining popliteal LNs and spleen was quantified using flow cytometry. CFSE-positive cells recovered from TDLNs are from “ipsilateral injection,” and CFSE-positive cells recovered from NTDLNs are from “contralateral injection” as depicted in Fig. 7A.

Over nine times more ipsilaterally injected labeled lymphocytes were recovered from the TDLN compared to the NTDLN (Fig. 7B). Very few labeled cells were recovered from the contralateral popliteal LNs (Fig. 7C), confirming that labeled cells entered the popliteal LNs via the afferent lymph rather than from the bloodstream. In TDLNs, entry of B cells from the afferent lymph was increased (Fig. 7D), as was the entry of non-B cells compared to NTDLNs (Fig. 7E). Afferent entry of B cells into TDLNs was increased 20-fold, compared to a 4-fold increase in non-B cell entry into TDLNs (Fig. 7F). Under homeostatic conditions, CD4<sup>+</sup> T cells enter peripheral LNs through afferent lymph more readily than other lymphocyte populations.<sup>35</sup> Similarly, in our experiment the proportion of injected CD4<sup>+</sup> T cells in NTDLNs was significantly larger than the comparable B cell and CD8<sup>+</sup> T cell populations in NTDLNs (Fig. 7G). Interestingly, the fractions of injected B cells, CD4<sup>+</sup> T cells, and CD8<sup>+</sup> T cells that entered the TDLNs were comparable (Fig. 7H), suggesting that tumor-driven alterations in lymph drainage affect trafficking of all types of lymphocytes to TDLNs.

### Enhanced retention of B cells in TDLNs involves reduced S1PR1 expression

We determined that decreased egress of B cells from TDLNs is a major contributor to the preferential accumulation of B lymphocytes in TDLNs. Lymphocyte trafficking through lymphoid tissue is directed by several chemokine signals,<sup>36,37</sup> including CXCL12,<sup>38</sup> CXCL13,<sup>39</sup> CCL19/21,<sup>39</sup> and the small lipid S1P.<sup>40</sup> We hypothesized that enhanced retention of B cells in TDLNs could be due to increased pro-retention chemokine signaling

**Figure 3.** (see previous page) Lymphocyte apoptosis is not significantly altered in TDLNs. (A) Representative histogram of activated (cleaved) caspase-3 in NTDLN and TDLN B and non-B lymphocytes in a mouse with footpad B16-F10 melanoma. (B) Total numbers of activated caspase-3-positive B lymphocytes in NTDLNs and TDLNs. There is a trend toward increased B cell apoptosis in TDLNs (B cells  $p = 0.08$ ). (C) Total numbers of activated caspase-3-positive non-B cells demonstrates a similar trend ( $p = 0.05$ ). (D) Total numbers of activated caspase-3-positive CD4<sup>+</sup> and (E) CD8<sup>+</sup> T cells from the non-B cell population analyzed in B. A trend toward increased CD4<sup>+</sup> and CD8<sup>+</sup> T cell apoptosis in TDLNs is evident (CD4<sup>+</sup> T cells  $p = 0.05$ , CD8<sup>+</sup> T cells  $p = 0.06$ ). (F) B lymphocyte and (G) non-B lymphocyte apoptosis is proportional to the size of these populations in NTDLNs and TDLNs (B cells  $p = 0.67$ , non-B cells  $p = 0.17$ ). (H) Similarly, CD4<sup>+</sup> and (I) CD8<sup>+</sup> T cell apoptosis is proportional to these populations in TDLNs compared to NTDLNs (CD4<sup>+</sup> T cells  $p = 0.17$ , CD8<sup>+</sup> T cells  $p = 0.19$ ). (n = 7 paired LN in three independent experiments, mean + SEM depicted).

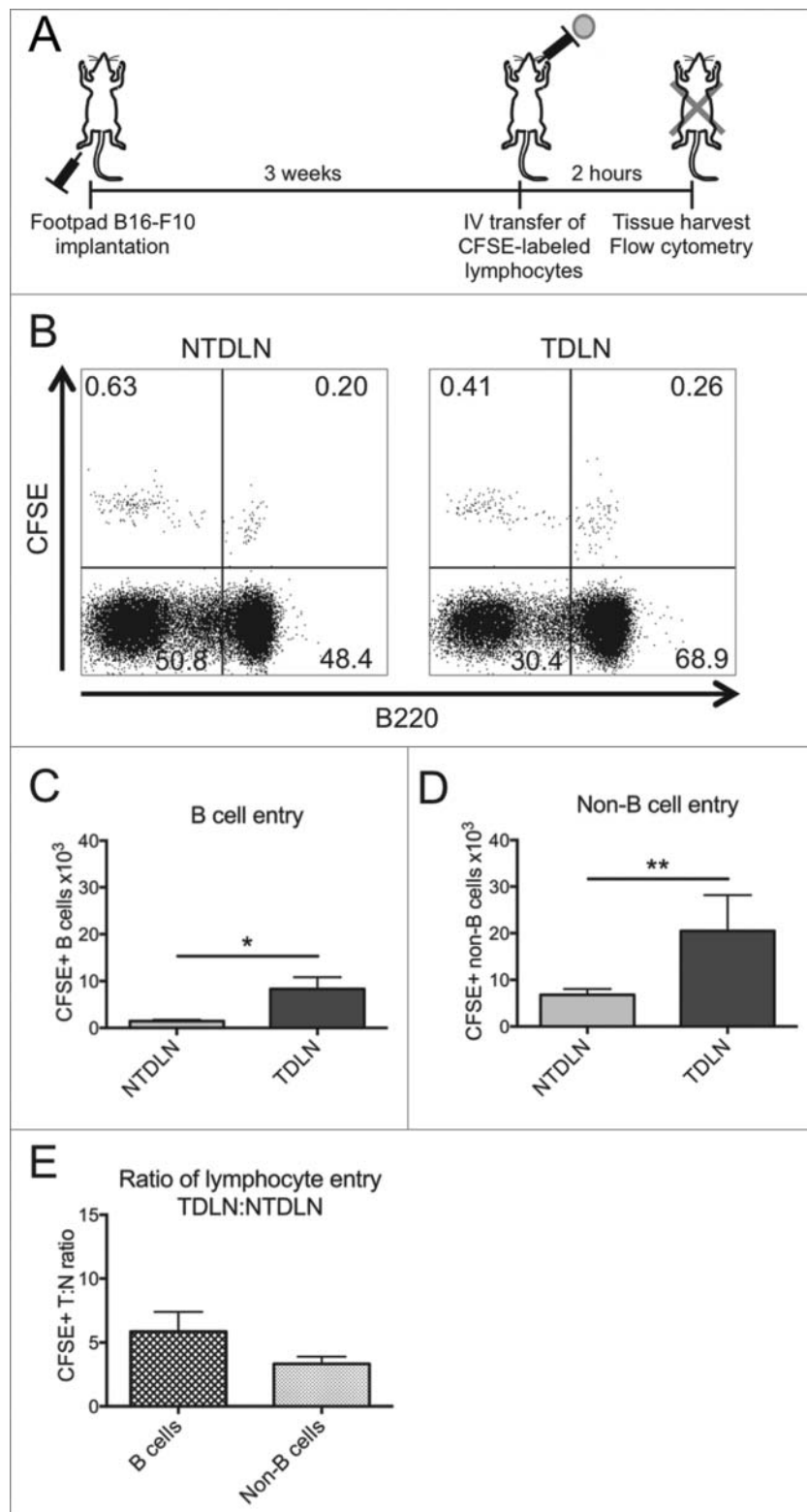


**Figure 4.** Lymphocyte entry via HEVs is increased in TDLNs, but does not fully account for preferential B cell accumulation. (A) Schematic diagram of an experiment to quantify CFSE-labeled lymphocyte entry into TDLNs via the bloodstream. (B) Representative dot plot of labeled lymphocytes within a NTDLN and TDLN 2 h after IV transfer. (C) Total numbers of labeled B cells and (D) non-B cells within NTDLNs and TDLNs 2 h after IV transfer. More B ( $p = 0.02$ ) and non-B ( $p = 0.008$ ) lymphocytes were recovered from TDLNs than NTDLNs. (E) Total numbers of labeled B and non-B lymphocytes, expressed as a ratio of these populations in TDLNs to NTDLNs, demonstrated no difference in LN entry between B and non-B cells ( $p = 0.13$ ). ( $n = 8$  paired LNs in two independent experiments, mean + SEM depicted).

(i.e., CXCR4/CXCL12, CXCR5/CXCL13, or CCR7/CCL19/21) or decreased exit signaling (i.e., S1PR1/S1P). To determine which of these signaling pathways are most important for TDLN B cell retention, the surface expression of chemokine

receptors on TDLN and NTDLN lymphocytes was determined using flow cytometry.

CXCL12 on HEVs plays an important role in lymphocyte recruitment to peripheral lymph nodes.<sup>41,42</sup> In addition,

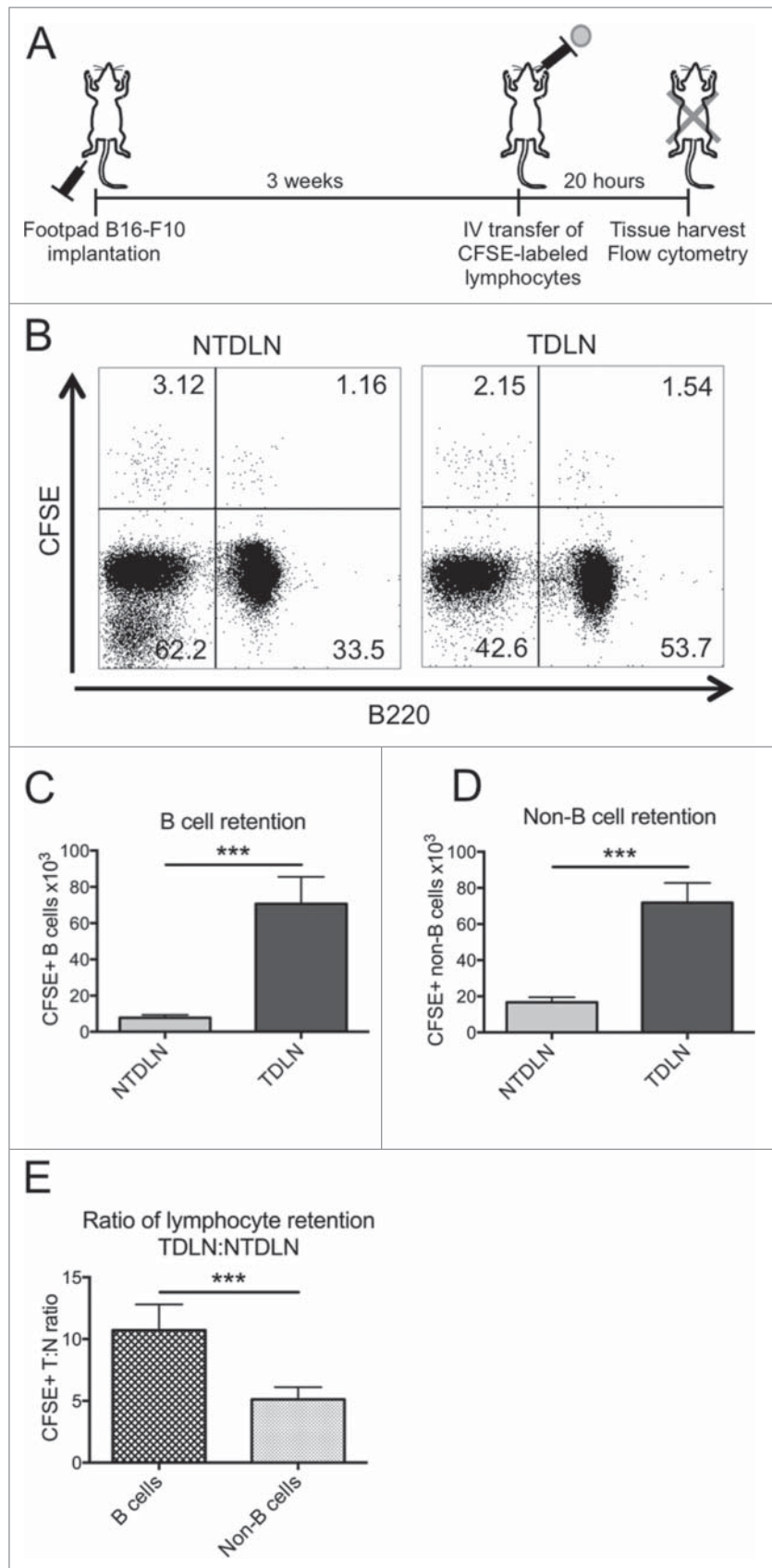


**Figure 5.** (B) cells are preferentially retained in TDLNs. (A) Schematic diagram of an experiment to quantify CFSE-labeled lymphocyte retention. (B) Representative dot plot of labeled lymphocytes in NTDLN and TDLN 20 h after IV transfer. (C) Total numbers of labeled B and (D) non-B lymphocytes 20 h after IV transfer. In TDLNs, an increased number of labeled B cells ( $p = 0.001$ ) and non-B cells ( $p = 0.0002$ ) has entered but not exited compared to NTDLNs. (E) Total numbers of retained labeled B and non-B lymphocytes at 20 h after IV transfer, expressed as a ratio between TDLN and NTDLN for each mouse. The ratio of retained B cells is greater in TDLNs than that of non-B cells ( $p = 0.001$ ). ( $n = 12$  paired LNs in two independent experiments, mean + SEM depicted).



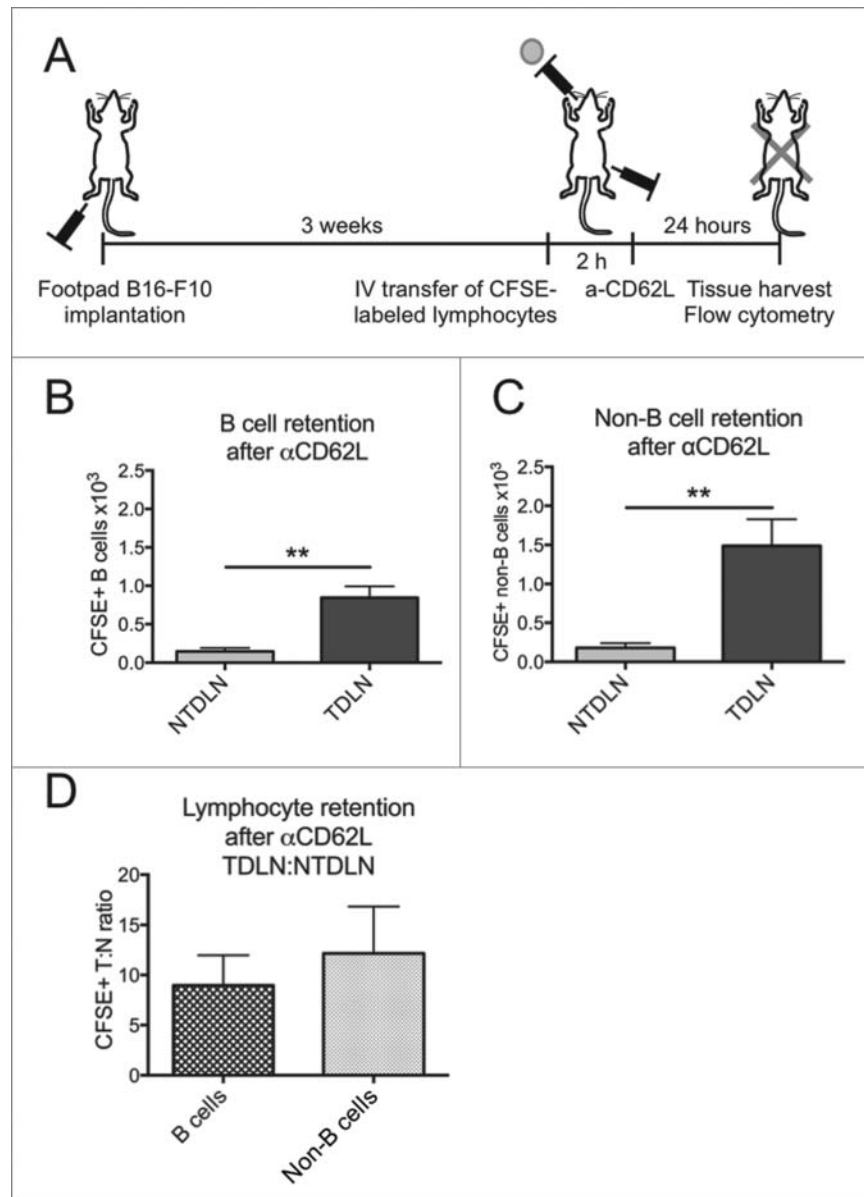


**Figure 6.** Timed lymphocyte entry into LNs confirms retention of lymphocytes in TDLNs. (A) Schematic diagram of an experiment to quantify retention of labeled lymphocytes in NTDLNs and TDLNs 24 h after a 2 h entry window. (B) Total numbers of retained labeled B lymphocytes and (C) non-B lymphocytes in NTDLNs and TDLNs 24 h after a 2 h entry window. B and non-B cells are retained in TDLNs compared to NTDLNs ( $p = 0.005$ ,  $p = 0.008$ , respectively). (D) Total numbers of retained labeled lymphocytes 24 h after a 2 h entry window, expressed as a ratio of TDLN to NTDLN for each mouse. Focusing on cells entering only within the first 2 h, B cell retention in TDLNs is similar to that observed in the first exit experiment (compare to Fig. 5E). Unexpectedly, an increased proportion of labeled non-B cells was recovered from NTDLN after arrest of lymphocyte entry via HEVs. ( $n = 6$  paired LNs in two independent experiments, mean + SEM depicted).

downregulation of its ligand, CXCR4, on B cells is reported to promote rapid depolarization of bone marrow-resident B cells and export into peripheral blood.<sup>43</sup> Therefore, we considered whether upregulation in CXCR4 surface expression could play a role in B cell retention in TDLNs. However, TDLN B cells exhibited reduced CXCR4 expression (Figs. 8A–C), suggesting that preferential B cell retention in TDLNs is not caused by increased CXCR4 signaling. Non-B cell surface expression of CXCR4 was unchanged in TDLNs compared to NTDLNs (Figs. 8A–C).

CXCL13 is produced by follicular dendritic cells within LN follicles, and is important for attracting B cells to LN follicles,<sup>36,44,45</sup> suggesting that increased CXCR5/CXCL13 signaling could prevent TDLN B cells from reaching lymphatic sinus exit sites. Instead, B cells in TDLNs exhibited decreased

CXCR5 surface expression (Figs. 8D and E). This suggests that increased CXCR5/CXCL13 signaling is not the mechanism of preferential B cell retention in TDLNs. Non-B cell surface expression of CXCR5 was low, and unchanged in TDLNs compared to NTDLNs (Figs. 8D–F).

The balance between CCR7 signaling and S1PR1 signaling is known to be a key determinant of T cell exit from secondary lymphoid tissues.<sup>46</sup> CCR7 signaling promotes T cell retention within the lymph node parenchyma, while S1PR1 signaling promotes egress into efferent lymph.<sup>40</sup> Surface expression of these receptors could also be important for B cell retention in LNs.<sup>47</sup> Surprisingly, we found an increase in the relative number of CCR7-negative B cells in TDLNs, as well as fewer CCR7-positive non-B cells (Figs. 8G–I). Together, this indicates that neither B cell nor

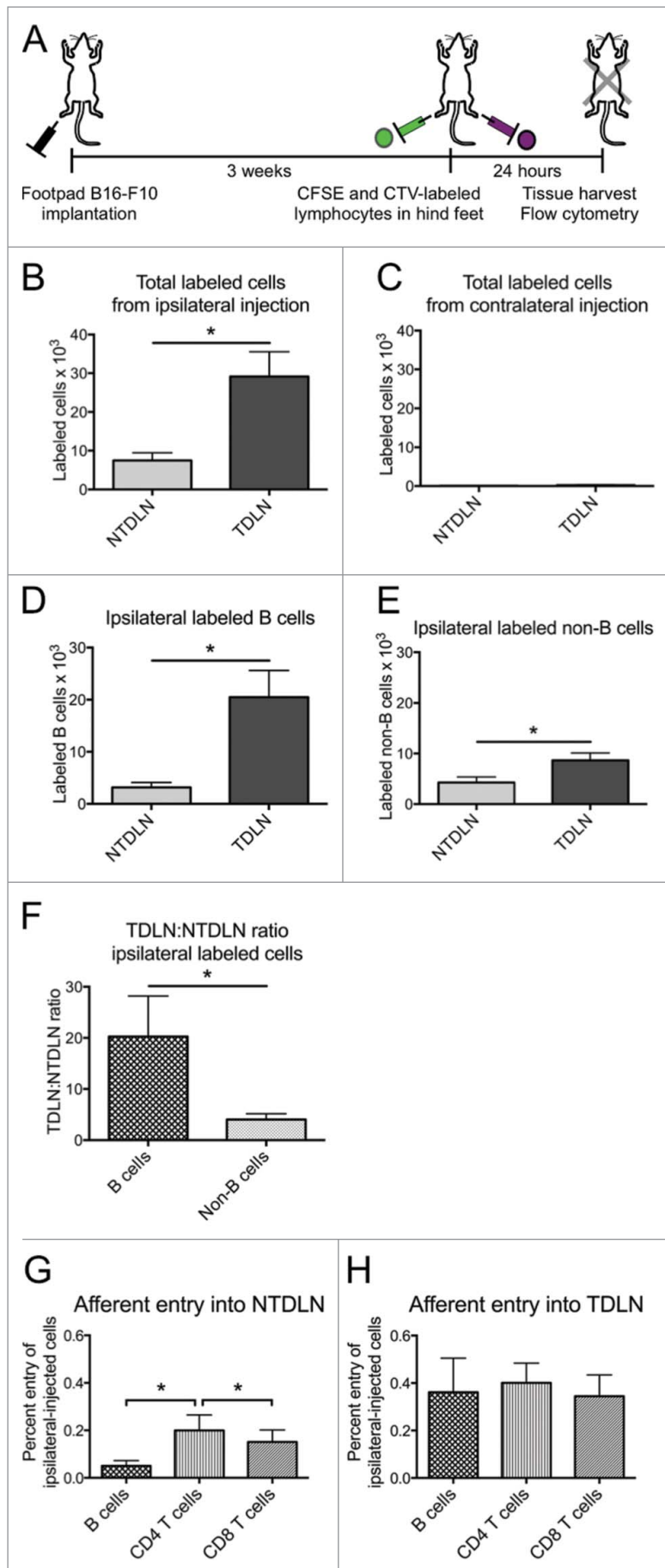


Figure 7. (For figure legend, see page 11.)

non-B cell retention in TDLNs is due to increased CCR7 surface expression.

Another important mediator of lymphocyte egress from LNs is S1PR1/S1P signaling. Similar to many chemokines, surface expression of S1PR1 is tightly regulated to respond to S1P gradients in fluids and tissues throughout the body.<sup>48</sup> Blood and lymph contain high extracellular S1P concentrations, whereas the parenchyma of secondary lymphoid organs exhibits low concentrations of S1P.<sup>40</sup> S1PR1 surface expression is low when lymphocytes follow other signals to enter the LN, and is upregulated while lymphocytes are exposed to the low S1P LN environment.<sup>49</sup> After exposure to antigens within the LN, high surface expression of S1PR1 on the lymphocyte facilitates their migration out of the LN via efferent lymph.<sup>50</sup> Decreased S1PR1 surface expression, as occurs with CD69<sup>+</sup> lymphocyte activation in acute inflammation, results in lymphocyte retention in LN.<sup>17,51</sup>

To test whether retention of lymphocytes in TDLNs could be mediated by S1PR1 signaling, expression of S1PR1 on lymphocytes from TDLNs and NTDLNs was assessed by flow cytometry (Fig. 9A). B cells in TDLNs feature decreased surface expression of S1PR1 (Fig. 9B), consistent with a decreased egress signal and subsequent retention in TDLNs. Non-B cell surface expression of S1PR1 was similar in TDLNs and NTDLNs (Fig. 9C). Fewer TDLN B cells were S1PR1-high than in NTDLNs (Fig. 9D), and S1PR1-high non-B cells were also decreased in TDLNs (Fig. 9E). These observations demonstrate that decreased S1PR1 expression could account for preferential retention of B cells in TDLNs, and could also contribute to TDLN T cell retention.

### Decreased S1PR1 surface expression in TDLN lymphocytes is not regulated by CD69

Direct interaction of S1PR1 with CD69 on activated lymphocytes can decrease S1PR1 surface expression,<sup>17,51</sup> which suggests a possible mechanism of lymphocyte activation driving S1PR1 downregulation on lymphocytes in TDLNs. CD69 is rapidly expressed following activation of B and T cells (reviewed in ref.<sup>52</sup>) CD8<sup>+</sup> T cell activation has been reported in TDLN lymphocytes using a flank B16-OVA melanoma model,<sup>25</sup> suggesting that activation could account for decreased S1PR1 surface expression on lymphocytes and reduced lymphocyte egress from TDLNs.

CD69 expression on TDLN and NTDLN lymphocytes was assessed using flow cytometry (Fig. 10A). Surprisingly, CD69 surface expression was decreased on TDLN B cells (Fig. 10B), and was unchanged on TDLN non-B cells (Fig. 10C). To test whether increased CD69 expression could be driving decreased S1PR1 surface expression, we directly compared CD69 MFI on high- and low-surface S1PR1-expressing lymphocytes. In fact, S1PR1-high lymphocytes also expressed higher amounts of CD69 than S1PR1-low lymphocytes. This pattern was consistent in B cells (Fig. 10D) and T cells (Fig. 10E) of TDLNs and NTDLNs. Together, these

findings demonstrate that downregulation of S1PR1 on TDLN lymphocytes is not directly regulated by CD69 expression.

## Discussion

The footpad B16-F10 melanoma model uniquely allowed intramouse comparison of factors influencing the accumulation of lymphocytes in TDLNs versus NTDLNs. This study identified multiple mechanisms that contribute to TDLN hypertrophy and differ between B and T cells. Compared to T cells, B cells are preferentially retained in TDLNs, corresponding with decreased S1PR1 expression on TDLN B cells, which is not mediated by increased CD69 expression. B cells trafficking from the tumor in afferent lymph also are more likely to enter TDLNs than T cells. We observed that within TDLNs, increases in B and T cell entry and proliferation were similar between cell types, and proportional to LN cellularity. These findings demonstrate that differences in lymphocyte egress are most important for creating a B-cell predominant TDLN population.

S1PR1 surface expression on lymphocytes exerts a key role in directing lymphocyte egress from LNs,<sup>53,54</sup> and is modulated by multiple mechanisms, only some of which have been extensively characterized.<sup>17,51,55</sup> CD69-independent lymphocyte sequestration caused by decreased S1PR1 expression of lymphocytes in draining LNs and Peyer's patches has previously been described in models of acute bacterial<sup>55</sup> or viral infection.<sup>56</sup> The same mechanism of CD69-independent S1PR1 downregulation could operate in our footpad melanoma model. In addition, high levels of S1P in TDLNs could potentially mediate lymphocyte S1PR1 downregulation. Surface expression of S1PR1 is low on circulating lymphocytes exposed to high S1P concentrations in lymph and blood, and gradually upregulated in low-S1P environments, such as within the parenchyma of LNs.<sup>40</sup> Surface expression of S1PR1 determines T lymphocyte egress kinetics.<sup>50</sup> Though tissue levels of S1P are tightly regulated in homeostasis, multiple mechanisms could lead to an increased S1P concentration in TDLNs. S1P is high in lymph, maintained by lymphatic endothelial cells.<sup>57,58</sup> The major expansion of lymph flow and lymphatic sinuses within these TDLNs could increase S1P levels within the LN compared to NTDLNs.<sup>3</sup> Interstitial S1P concentrations are elevated in many cancers (summarized in ref.<sup>59</sup>), which could further elevate the S1P concentration of lymph draining from tumors to increase the parenchymal concentration of S1P in TDLNs, blunting the response of TDLN lymphocytes to this exit-signaling molecule. New techniques to quantify S1P with high spatial resolution will be needed to evaluate this hypothesis, given the many challenges of quantifying S1P *in vivo* (summarized in ref.<sup>40</sup>).

An inverse relationship between S1PR1 receptors and the activation marker CD69 has been described in several models of infection and inflammation, with direct interaction between

**Figure 7.** (see previous page) Lymphocyte entry into TDLNs via afferent lymph is increased compared to NTDLNs. (A) Schematic diagram of an experiment to quantify lymphocyte entry into TDLNs and NTDLNs via afferent lymph. (B) Total number of labeled lymphocytes recovered from NTDLNs and TDLNs following ipsilateral SC injection into the dorsal toe of unilateral footpad B16-F10 melanoma bearing mice. More labeled cells were recovered from the ipsilateral TDLNs than NTDLNs ( $p = 0.01$ ). (C) Few cells were recovered in TDLNs or NTDLNs from contralateral foot injections, indicating that labeled cells entered via afferent lymph rather than the bloodstream. (D) Total number of cells in (B) divided into B ( $p = 0.01$ ) and (E) non-B cells ( $p = 0.04$ ). (F) Total numbers of labeled B and non-B lymphocytes in (C), expressed as ratio of TDLNs to NTDLNs. The ratio of labeled B cells was significantly higher than that of labeled non-B cells recovered in draining lymph nodes ( $p = 0.04$ ). (G) Recovered labeled lymphocyte populations from NTDLNs and (H) TDLNs broken down into B and T cell subsets. Unlike naive T cell entry into NTDLNs via afferent lymphatics, no preferential entry of labeled CD4<sup>+</sup> T cells was observed in TDLNs. ( $n = 6$  paired LNs in two independent experiments, mean + SEM depicted).

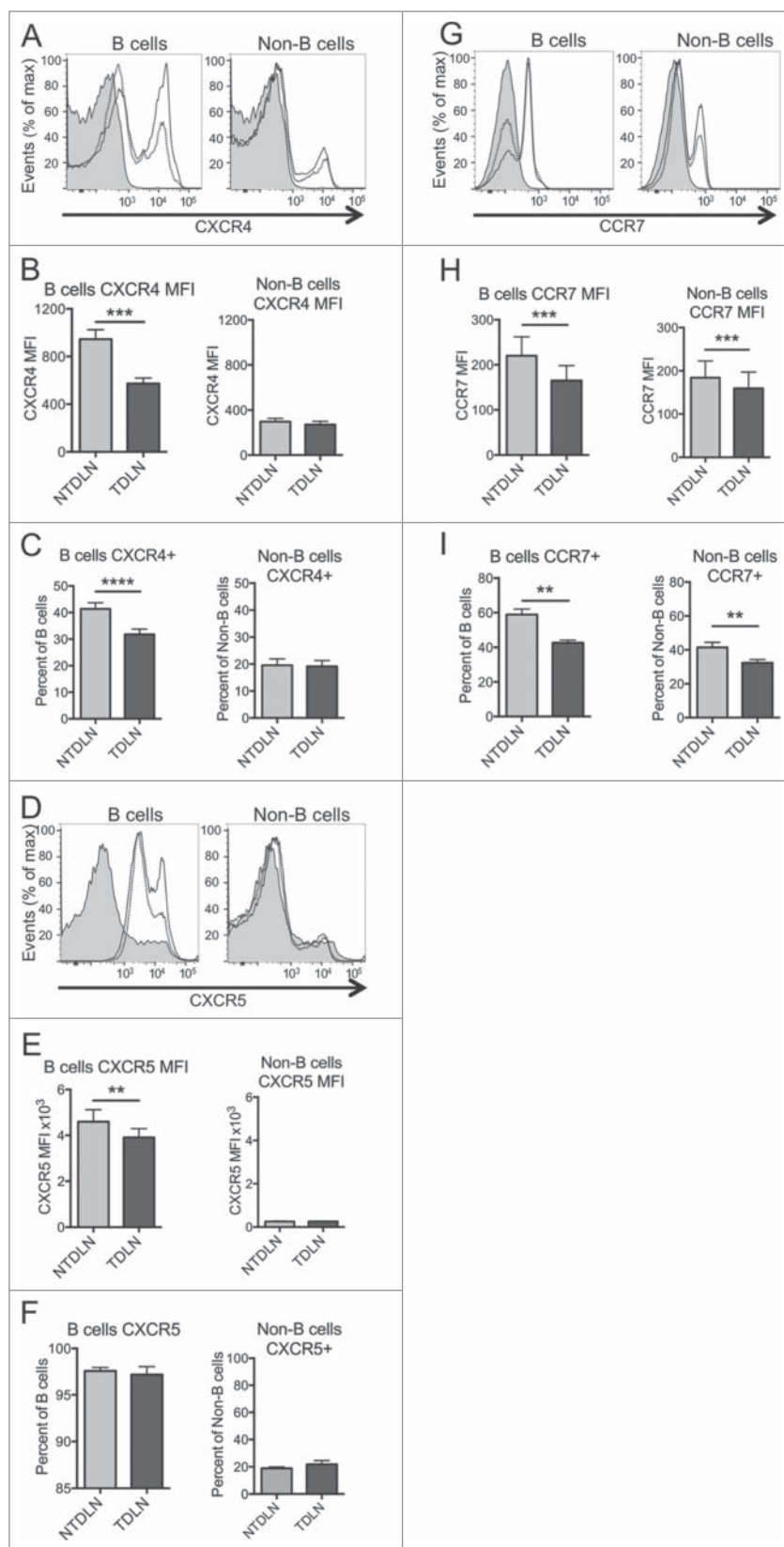


**Figure 8.** Decreased chemokine receptor expression does not account for lymphocyte retention in TDLNs. Representative histograms of (A) CXCR4, (D) CXCR5, (G) CCR7 surface expression on B and non-B lymphocytes of NTDLNs (solid line) and TDLNs (dashed line). Filled curve is isotype control. B cells have decreased (B) CXCR4 ( $p = 0.0002$ ) and (E) CXCR5 ( $p = 0.004$ ) surface expression. On non-B cells, surface expression of (C) CXCR4 and (F) CXCR5 are unchanged. The CXCR5 isotype demonstrated low-level background staining in both TDLN and NTDLN samples, and so did not affect analysis for any one population. (H) Both B and non-B cells have lower CCR7 expression in TDLNs ( $p = 0.0007$  and  $p = 0.0009$ , respectively). (I) CCR7-negative B cell populations are increased in TDLNs ( $p = 0.003$ ), and fewer non-B cells are CCR7-positive in TDLNs ( $p = 0.0099$ ). (CXCR4, CCR7  $n = 9$  paired LN in three independent experiments; CXCR5  $n = 11$  paired LN in three independent experiments, mean + SEM depicted).



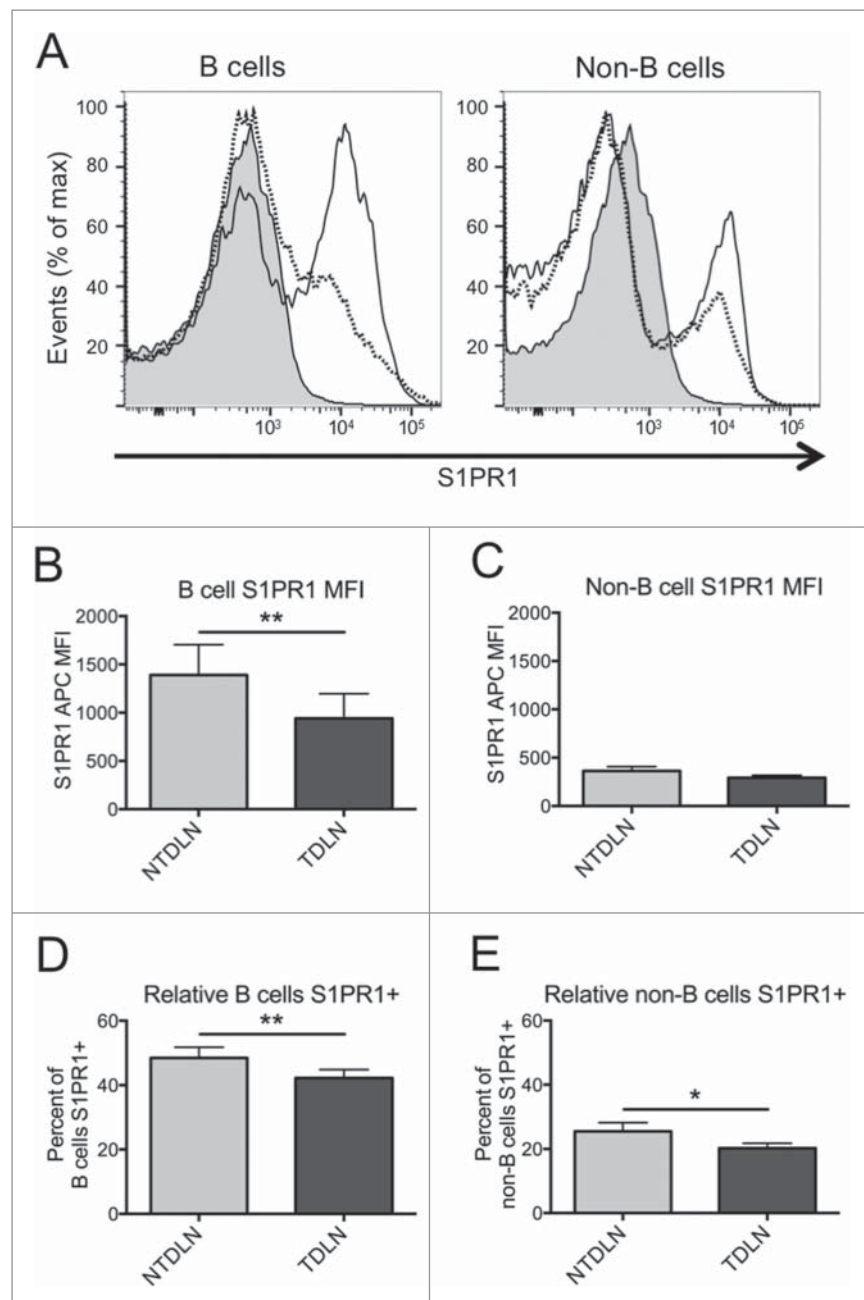


**Figure 9.** Reduced lymphocyte S1PR1 is consistent with decreased egress from TDLNs. (A) Representative histogram of surface S1PR1 in B and non-B lymphocytes in NTDLN (solid line) and TDLN (dotted line) of a mouse with footpad B16-F10 melanoma. Filled curve is the isotype control. (B) Mean fluorescence intensity (MFI) of S1PR1 on B and (C) non-B lymphocytes in NTDLNs and TDLNs. B cell S1PR1 is decreased ( $p = 0.006$ ), whereas non-B cell S1PR1 is not significantly changed ( $p = 0.11$ ). (D) The percentage of S1PR1-high expressing B lymphocytes is decreased in TDLN ( $p = 0.007$ ). (E) The percentage of S1PR1-high expressing non-B lymphocytes is also decreased in TDLNs ( $p = 0.03$ ). ( $n = 9$  paired LN in three independent experiments, mean + SEM depicted).

the two proteins.<sup>17,51,60</sup> After observing that S1PR1 surface expression is decreased in TDLN B cells, we expected to find increased lymphocyte activation and CD69 expression, which could be consistent with activation of an antitumor immune response. Instead, CD69 surface expression on lymphocytes in TDLNs was low and comparable to normal NTDLNs, consistent with a minimal immune response to the B16-F10 melanoma.<sup>61</sup> This demonstrates that lymphocyte activation does not play a major role in retention of TDLN lymphocytes in this model. In contrast, other studies have found a more prominent role of tumor-driven lymphocyte activation, including the appearance of CD69-positive T lymphocytes in mice bearing

large OVA foreign antigen-expressing B16-F10 subcutaneous, lung, and intraperitoneal tumors.<sup>25,62</sup> It is possible that the degree of lymphocyte activation is antigen and/or stage-dependent. In those tumor models, CD69-positive activation could be predicted to further diminish S1PR1-mediated exit signals for lymphocytes, further enhancing lymphocyte accumulation in TDLNs and promoting tumor growth and progression. Surface expression of S1PR1 on TDLN lymphocytes may be modified by additional transcriptional or post-transcriptional mechanisms, an interesting area of future research.<sup>63</sup>

Multiple studies have suggested that immunosuppressive drugs targeting S1P/S1PR signaling, such as FTY720 (fingolimod,

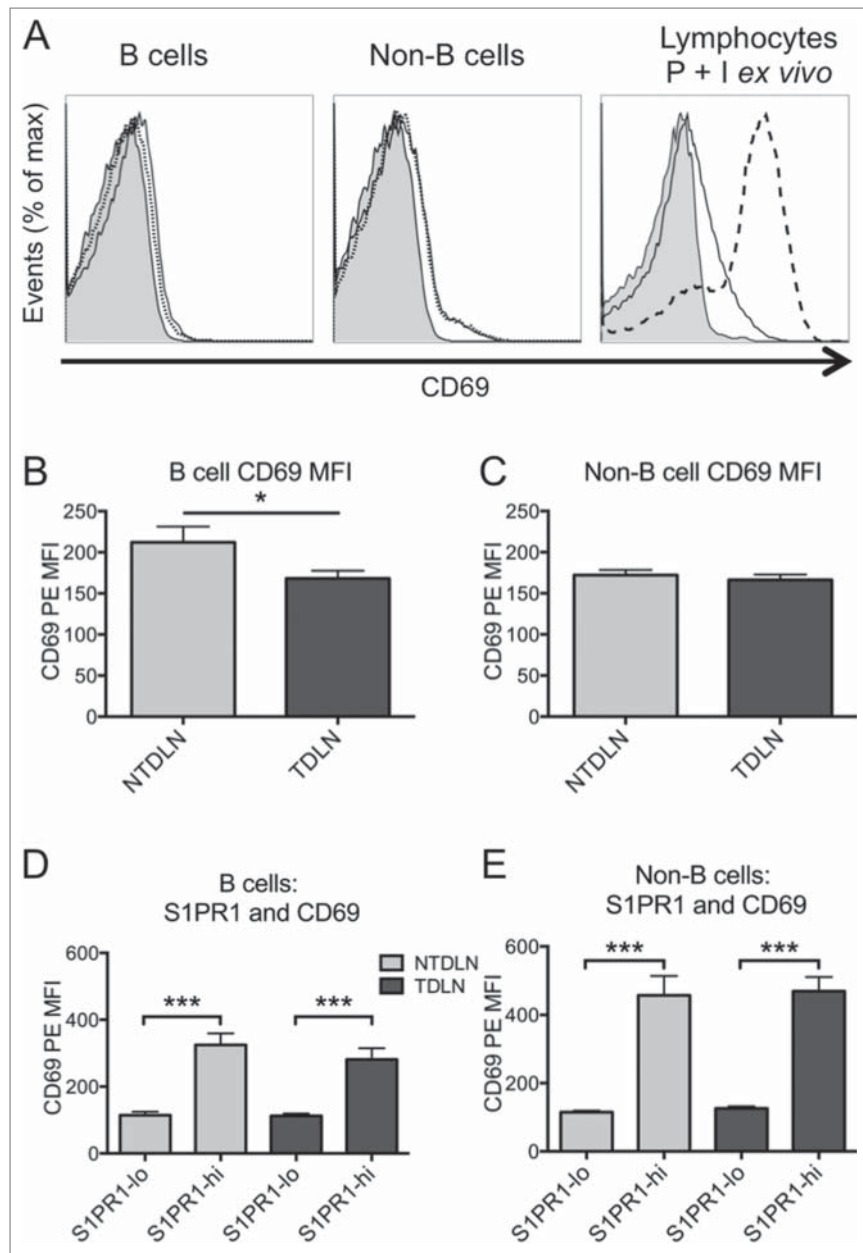


**Figure 10.** TDLN lymphocytes exhibit low levels of CD69 activation marker expression. (A) Representative histogram of CD69 expression on B and non-B lymphocytes in a NTDLN (solid line), TDLN (dotted line), and naive splenocytes stimulated *in vitro* with PMA + ionomycin as positive control (dashed line). Filled curve is isotype control. (B) Mean fluorescence intensity of CD69 expression on B lymphocytes ( $p = 0.03$ ) and (C) non-B lymphocytes ( $p = 0.5$ ) in NTDLNs and TDLNs. (D) Relationship between low and high expression of S1PR1 and CD69 expression on B and (E) non-B lymphocytes from NTDLNs and TDLNs. Note consistent positive correlation between expression levels of S1PR1 and CD69 ( $p = 0.0001$ ). (n = 8 paired LN in three independent experiments, mean + SEM depicted).

Gilenva) (summarized in ref.<sup>64</sup>) and SpHINGOMAB<sup>65</sup> may be useful adjunctive antitumor therapies. Several mechanisms are implicated in the observed effects on tumor cells and cancer outcome, including regulation of new blood vessel formation, direct cellular toxicity, and regulation of cellular survival and metabolism.<sup>64,65</sup> Understanding the role of S1P signaling in TDLNs could lead to better-targeted antitumor therapies that promote lymphocyte egress to allow an antitumor immune response.

Unlike the response of draining LNs to inflammation,<sup>30,66</sup> increased entry of lymphocytes via HEVs does not appear to be the primary mechanism of TDLN hypertrophy, although it does contribute to overall lymphocyte accumulation. In this study, neither B nor T lymphocyte entry was preferentially activated in TDLNs, suggesting that entry continues proportionate to the expansion of

HEVs in the expanding TDLNs.<sup>3</sup> Though it has been suggested that lymphocyte entry to TDLNs is altered, to our knowledge this is the first experimental quantification of this mechanism.

An unexpected finding of our study was the effect of tumors to enhance trafficking of naive B and T lymphocytes into TDLNs via afferent lymphatic vessels. Afferent lymphatic uptake of T cells and dendritic cells has only recently been characterized,<sup>26,67,68</sup> and has long been thought to be a minor contributor to LN cell populations, based on lymphatic cannulation studies performed in sheep.<sup>32,69</sup> Recent studies in mice have demonstrated that inflammation promotes trafficking of lymphocytes within afferent lymph to draining LNs, dependent on chemokine signals.<sup>67,68,70,71</sup> Tumor-resident T cells have been associated with the promotion of an antitumor immune response, and are utilized in cellular tumor

immunotherapy.<sup>72</sup> Lymphatic trafficking of tumor-educated T cells to TDLNs could serve to stimulate or repress the antitumor immune response, depending on the interactions of those cells within the TDLN.<sup>70</sup> The observed disproportionate increases in entry of CD8<sup>+</sup> T cells and B cells into TDLNs compared to normal LNs<sup>35</sup> and NTDLNs (our study) highlight the profound impacts of the tumor on afferent lymphatic trafficking of lymphocytes. Our finding that lymphocytes have an increased propensity to enter TDLNs via afferent lymph could inspire new approaches to manipulate antitumor immune responses.

Surprisingly, naive B cells in the subcutaneous space draining the tumor-bearing foot were 20 times more likely to enter the TDLN than the NTDLN in our model. The physiologic relevance of this finding for the footpad B16-F10 model is unknown. Trafficking of naive B cells through peripheral tissues and afferent lymphatic drainage has recently been described in mice.<sup>68,73</sup> B cells have not been detected in B16-F10 footpad melanomas,<sup>3</sup> suggesting that this mechanism is not a major contributor to preferential accumulation of B cells in TDLNs of this model. However, increased B cell trafficking via afferent lymphatics may have important implications for other types of tumors that harbor significant B cell populations.<sup>74-76</sup> Further studies are needed to track lymphocytes entering LNs via the afferent lymph, to determine whether they return to the tumor as effector cells, or if they contribute to tumor tolerance within the TDLN.

Remodeling of TDLN architecture may also contribute to the generation of TDLN hypertrophy due to the extensive growth of lymphatic sinuses, which spread throughout the LN cortex and medulla,<sup>3,4</sup> while the accumulating B cells infiltrate the paracortical T cell zone. These architectural changes could be related to the reduction of chemokine receptor expression we identified in TDLN lymphocytes. This could reduce the affinity for chemokine ligands within TDLNs that normally direct lymphocyte position within the LN, to increase lymphocyte residence time in TDLNs.<sup>28</sup> For example, decreased CXCR5 on B cells may make these cells less responsive to CXCL13 produced by follicular dendritic cells.<sup>45</sup> Without a strong chemotactic attraction to CXCL13 in the cortical follicles, TDLN B cells may not make the necessary cellular contacts to respond to tumor-derived antigens, upregulate S1PR1, and/or to leave the LN via normal lymphatic sinus exit sites. Beta-adrenergic signaling within LNs can also block lymphocyte egress from LNs,<sup>77</sup> although further research is needed to test this potential contribution. Moreover, the expanded lymphatic sinuses throughout TDLNs could provide enhanced opportunities for the retained lymphocytes to undergo or develop anergy via incomplete antigen stimulation without appropriate co-stimulatory signaling, as a mechanism to promote tumor tolerance.<sup>78,79</sup> Though the majority of B cells in TDLNs carry markers of follicular B cells, regulatory B cells preferentially accumulate, and may drive tumor tolerance in TDLNs.<sup>16</sup> Additional studies will be needed to characterize the mechanisms of preferential accumulation of regulatory B cell populations in TDLNs.

The identification of multiple mechanisms regulating TDLN lymphocyte accumulation suggests promising avenues to improve antitumor immunotherapy. For example, strategies to reduce lymphocyte entry via the lymphatics and/or to limit retention of B cells could prevent accumulation of tumor-tolerizing Breg cells.<sup>12</sup>

Alternatively, strategies to re-establish a normal S1P gradient in TDLNs could facilitate B cell egress, prevent lymphangiogenesis in TDLNs, and slow metastasis.<sup>53,59,80</sup>

## Materials and methods

### Mouse melanoma model

C57BL/6J mice were obtained from the Jackson Laboratory (Bar Harbor, ME) and housed in sterile micro-isolator cages under specific pathogen-free conditions at the Fred Hutchinson Cancer Research Center or at a University of Washington centralized animal facility. Four to six week-old mice were injected subcutaneously in the right or left hind footpad with 180,000 B16-F10 cells (American Type Culture Collection) in 40  $\mu$ L of Hanks' buffered saline solution (HBSS; Gibco Life Technologies). The contralateral hind footpad was injected with sterile HBSS as vehicle control. B16-F10 cells were tested to confirm that the cells were free of mycoplasma contamination (MycoAlert). Mice were euthanized on 19–23 d post-tumor implantation for downstream analyses. The FHCRC and UW Animal Care and Use Committees approved all animal handling and procedures.

### Proliferation analysis

One percent bromodeoxyuridine (BrdU) in sterile phosphate-buffered saline (PBS) was administered IP to B16-F10 melanoma footpad tumor-bearing mice 17 h prior to euthanasia and tissue harvest. A single-cell suspension of lymphocytes isolated from the left and right popliteal lymph nodes were fixed and permeabilized (BD Cytofix/Cytoperm) before and after one freeze-thaw cycle at  $-80^{\circ}\text{C}$ . The cells were treated with 0.03% DNase in Dulbecco's phosphate-buffered saline solution to expose incorporated BrdU and stained with fluorescent-tagged antibodies prior to flow cytometry analysis as described below.

### Apoptosis analysis

Lymphocytes isolated from C57BL/6J popliteal lymph nodes from B16-F10 bearing mice as described above were stained with caspase-3/7 Detection Reagent (Life Technologies), followed by surface staining for B220, CD3, CD4<sup>+</sup>, and CD8<sup>+</sup> prior to flow cytometry analysis as described below.

### Lymph node entry and exit analysis

Spleens harvested from age-matched C57BL/6J mice were pooled and homogenized through a 70- $\mu$ m nylon filter (BD Biosciences). Single-cell suspensions were depleted of erythrocytes, resuspended at  $25 \times 10^6$  cells/mL 0.1% bovine serum albumin in PBS, and incubated for 10 min at  $37^{\circ}\text{C}$  in the presence of 0.8  $\mu$ M (entry) or 5  $\mu$ M (exit) 5,6-carboxyfluorescein diacetate succinimidyl ester (CFSE; Molecular Probes) prepared as a 5  $\mu$ M stock solution in dimethyl sulfoxide (DMSO). Cells were washed twice with Iscove's Modified Dulbecco's Medium (IMDM) supplemented with 10% fetal bovine serum, 4 mM L-glutamine, and 55  $\mu$ M of 2-mercaptoethanol. Cells were washed in Hank's buffered saline solution (HBSS) and resuspended at  $200 \times 10^6$  cells/mL. Each recipient mouse received  $40 \times 10^6$  CFSE-labeled cells intravenously. LNs were harvested 2 h or 20 h post-injection via flow cytometry

described below. To prevent continued entry of labeled lymphocytes in some exit experiments, mice were adoptively transferred CFSE-labeled cells as described above, followed by IP injection of 80  $\mu\text{g}$  anti-mouse CD62L-blocking antibody (BioLegend) after 2 h of equilibration, LN harvest 26 h after transfer of labeled cells, and flow cytometry.

### Afferent lymphocyte entry

Spleens harvested from age-matched C57BL/6J mice were pooled and homogenized through a 70- $\mu\text{m}$  nylon filter (BD Biosciences). Single-cell suspensions were depleted of erythrocytes, resuspended at  $25 \times 10^6$  cells/mL 0.1% BSA/PBS, and incubated for 10 min at 37°C in the presence of 5  $\mu\text{M}$  5,6-carboxyfluorescein diacetate succinimidyl ester (CFSE; Molecular Probes) or CellTrace Violet (Molecular Probes) prepared as a 5  $\mu\text{M}$  stock solution in DMSO. Cells were washed twice with Roswell Park Memorial Institute medium (RPMI) supplemented with 5% fetal bovine serum, 2 mM L-glutamine, 55  $\mu\text{M}$  2-mercaptoethanol, 1 mM pyruvate, 100 mM 4-(2-hydroxyethyl)-1-piperazineethanesulfonic acid (HEPES), 100 U/mL penicillin, 100 U/mL streptomycin. Cells were washed in Hanks' buffered saline solution (HBSS) and resuspended at  $400 \times 10^6$  cells/mL. Anesthetized mice were injected with  $8.0 \times 10^6$  CellTrace Violet-labeled cells in the subcutaneous space of the dorsal toe of the control (non-tumor-bearing) side, and  $8.0 \times 10^6$  CFSE-labeled cells in the dorsal toe of the tumor-bearing foot. Cells were allowed to traffic from the injection sites for 24 h before mouse euthanasia and tissue harvest. Lymphocytes harvested from the popliteal lymph nodes and spleen were analyzed by flow cytometry as described below.

### Lymphocyte activation

As a positive control for lymphocyte CD69 surface expression, splenocytes were cultured for 5 h at  $4 \times 10^6$  cells/mL in complete lymphocyte media (RPMI + 5% fetal bovine serum, 55  $\mu\text{M}$  2-mercaptoethanol, 1 mM pyruvate, 100 mM HEPES, 100 U/mL penicillin, 100 U/mL streptomycin) with phorbol 12-myristate 13-acetate (PMA, 2.5 ng/mL) + ionomycin (1.25 ng/mL) or without PMA + ionomycin as an un-stimulated control. Cells were analyzed by flow cytometry to assess surface marker expression.

### Flow cytometry analysis

Lymphocytes isolated from C57BL/6J popliteal lymph nodes by manual dissociation through a 35  $\mu\text{m}$  filter were stained extracellularly by incubation with  $\alpha$ -mouse B220-APC, -PerCPCy5.5, or -AF488 (BioLegend, San Diego, CA), IgM-eFluor<sup>®</sup> 450 (eBioscience), CD3 $\epsilon$ -APC/Cy7 or -APCeFluor780 (eBioscience), S1PR1-APC (R&D Systems), CD4<sup>+</sup>-PE (BioLegend), CD8<sup>+</sup>-AF488, -APC or -PacBlue (BioLegend), BrdU-FITC (Invitrogen), CD69-PE (BioLegend), CXCR4-PerCP-eFluor<sup>®</sup> 710 (eBioscience), CXCR5-APC (BioLegend), and CCR7-e450 (eBioscience) conjugated antibodies. Stained cells were fixed and acquired with a Canto II or LSR II cytometer (BD Biosciences) and analyzed using FlowJo software (Tree Star). At least 50,000 lymphocytes were analyzed for

each sample. Lymphocytes were identified by forward/side scatter profiles as depicted in Fig. 1.

### Statistics

All experiments were repeated two to three times with at least three mice per cohort. Statistical analyses were performed using GraphPad Prism 6 and were carried out using paired T tests or ANOVA.

### Disclosure of potential conflicts of interest

No potential conflicts of interest were disclosed.

### Acknowledgements

The authors thank Kim Jordan-Williams and Sheila Ganti for their advice, and Alexandra Croft for technical support.

### Funding

This work was supported by grants from NIH-NCI R01 CA68328 (AR), NIH R25 OD 010450 (LH), and NIH NCI T32 CA080416 (TA).

### References

- Schwartz LH, Bogaerts J, Ford R, Shankar L, Therasse P, Gwyther S, Eisenhauer EA. Evaluation of lymph nodes with RECIST 1.1. *Eur J Cancer* 2009; 45:261-7; PMID:19091550; <http://dx.doi.org/10.1016/j.ejca.2008.10.028>
- Van den Eynden GG, Van der Auwera I, Van Laere SJ, Huygelen V, Colpaert CG, van Dam P, Dirix LY, Vermeulen PB, Van Marck EA. Induction of lymphangiogenesis in and around axillary lymph node metastases of patients with breast cancer. *Br J Cancer* 2006; 95:1362-6; PMID:17088912; <http://dx.doi.org/10.1038/sj.bjc.6603443>
- Harrell MI, Iritani BM, Ruddell A. Tumor-induced sentinel lymph node lymphangiogenesis and increased lymph flow precede melanoma metastasis. *Am J Pathol* 2007; 170:774-86; PMID:17255343; <http://dx.doi.org/10.2353/ajpath.2007.060761>
- Qian CN, Berghuis B, Tsarfaty G, Bruch M, Kort EJ, Ditlev J, Tsarfaty I, Hudson E, Jackson DG, Petillo D et al. Preparing the "soil": the primary tumor induces vasculature reorganization in the sentinel lymph node before the arrival of metastatic cancer cells. *Cancer Res* 2006; 66:10365-76; PMID:17062557; <http://dx.doi.org/10.1158/0008-5472.CAN-06-2977>
- Ruddell A, Kelly-Spratt KS, Furuya M, Parghi SS, Kemp CJ. p19/Arf and p53 suppress sentinel lymph node lymphangiogenesis and carcinoma metastasis. *Oncogene* 2008; 27:3145-55; PMID:18059331; <http://dx.doi.org/10.1038/sj.onc.1210973>
- Farzad Z, Cochran AJ, McBride WH, Gray JD, Wong V, Morton DL. Lymphocyte subset alterations in nodes regional to human melanoma. *Cancer Res* 1990; 50:3585-8; PMID:1692763.
- Kohrt HE, Nouri N, Nowels K, Johnson D, Holmes S, Lee PP. Profile of immune cells in axillary lymph nodes predicts disease-free survival in breast cancer. *PLoS Med* 2005; 2:e284; PMID:16124834; <http://dx.doi.org/10.1371/journal.pmed.0020284>
- Ruddell A, Mezquita P, Brandvold KA, Farr A, Iritani BM. B lymphocyte-specific c-Myc expression stimulates early and functional expansion of the vasculature and lymphatics during lymphomagenesis. *Am J Pathol* 2003; 163:2233-45; PMID:14633598; [http://dx.doi.org/10.1016/S0002-9440\(10\)63581-X](http://dx.doi.org/10.1016/S0002-9440(10)63581-X)
- Hirota K, Wakisaka N, Sawada-Kitamura S, Kondo S, Endo K, Tsuji A, Murono S, Yoshizaki T. Lymphangiogenesis in regional lymph nodes predicts nodal recurrence in pathological N0 squamous cell carcinoma of the tongue. *Histopathology* 2012; 61:1065-71; PMID:22957497; <http://dx.doi.org/10.1111/j.1365-2559.2012.04341.x>



10. Jakob C, Aust DE, Liebscher B, Baretton GB, Datta K, Muders MH. Lymphangiogenesis in regional lymph nodes is an independent prognostic marker in rectal cancer patients after neoadjuvant treatment. *PLoS One* 2011; 6:e27402; PMID:22087309; <http://dx.doi.org/10.1371/journal.pone.0027402>
11. Van den Eynden GG, Vandenbergh MK, van Dam PJ, Colpaert CG, van Dam P, Dirix LY, Vermeulen PB, Van Marck EA. Increased sentinel lymph node lymphangiogenesis is associated with nonsentinel axillary lymph node involvement in breast cancer patients with a positive sentinel node. *Clin Cancer Res* 2007; 13:5391-7; PMID:17875768; <http://dx.doi.org/10.1158/1078-0432.CCR-07-1230>
12. Ganti SN, Albershardt TC, Iritani BM, Ruddell A. Regulatory B cells preferentially accumulate in tumor-draining lymph nodes and promote tumor growth. *Sci Rep* 2015; 5:12255; PMID:26193241; <http://dx.doi.org/10.1038/srep12255>
13. Ruddell A, Harrell MI, Furuya M, Kirschbaum SB, Iritani BM. B lymphocytes promote lymphogenous metastasis of lymphoma and melanoma. *Neoplasia* 2011; 13:748-57; PMID:21847366; <http://dx.doi.org/10.1593/neo.11756>
14. Moussion C, Girard JP. Dendritic cells control lymphocyte entry to lymph nodes through high endothelial venules. *Nature* 2011; 479:542-6; PMID:22080953; <http://dx.doi.org/10.1038/nature10540>
15. Cahill RN, Frost H, Trnka Z. The effects of antigen on the migration of recirculating lymphocytes through single lymph nodes. *J Exp Med* 1976; 143:870-88; PMID:1255114; <http://dx.doi.org/10.1084/jem.143.4.870>
16. Angeli V, Ginhoux F, Llodra J, Quemeneur L, Frenette PS, Skobe M, Jessberger R, Merad M, Randolph GJ. B cell-driven lymphangiogenesis in inflamed lymph nodes enhances dendritic cell mobilization. *Immunity* 2006; 24:203-15; PMID:16473832; <http://dx.doi.org/10.1016/j.immuni.2006.01.003>
17. Shioh LR, Rosen DB, Brdickova N, Xu Y, An J, Lanier LL, Cyster JG, Matloubian M. CD69 acts downstream of interferon- $\alpha/\beta$  to inhibit S1P1 and lymphocyte egress from lymphoid organs. *Nature* 2006; 440:540-4; PMID:16525420; <http://dx.doi.org/10.1038/nature04606>
18. Bertschmann M, Markwalder-Hartenbach R, Pedrinis E, Hess MW, Cottier H. Proliferative patterns of lymphocytes in lymph nodes during tumour development: involvement of T and B cell areas. *Br J Cancer* 1984; 49:477-84; PMID:6424695; <http://dx.doi.org/10.1038/bjc.1984.75>
19. Mueller SN, Jones CM, Smith CM, Heath WR, Carbone FR. Rapid cytotoxic T lymphocyte activation occurs in the draining lymph nodes after cutaneous herpes simplex virus infection as a result of early antigen presentation and not the presence of virus. *J Exp Med* 2002; 195:651-6; PMID:11877488; <http://dx.doi.org/10.1084/jem.20012023>
20. Cochran A, Huang R, Lee J, Itakura E, Leong S, Essner R. Tumour-induced immune modulation of sentinel lymph nodes. *Nat Rev Immunol* 2006; 6:659-70; PMID:16932751; <http://dx.doi.org/10.1038/nri1919>
21. Preynat-Seauve O, Contassot E, Schuler P, Piguet V, French LE, Huard B. Extralymphatic tumors prepare draining lymph nodes to invasion via a T-cell cross-tolerance process. *Cancer Res* 2007; 67:5009-16; PMID:17510433; <http://dx.doi.org/10.1158/0008-5472.CAN-06-4494>
22. Lund AW, Duraes FV, Hirosue S, Raghavan VR, Nembrini C, Thomas SN, Issa A, Hugues S, Swartz MA. VEGF-C Promotes Immune Tolerance in B16 Melanomas and Cross-Presentation of Tumor Antigen by Lymph Node Lymphatics. *Cell Rep* 2012; 1:191-9; PMID:22832193; <http://dx.doi.org/10.1016/j.celrep.2012.01.005>
23. Tewalt EF, Cohen JN, Rouhani SJ, Engelhard VH. Lymphatic endothelial cells - key players in regulation of tolerance and immunity. *Front Immunol* 2012; 3:305; PMID:23060883; <http://dx.doi.org/10.3389/fimmu.2012.00305>
24. Marzo AL, Lake RA, Lo D, Sherman L, McWilliam A, Nelson D, Robinson BW, Scott B. Tumor antigens are constitutively presented in the draining lymph nodes. *J Immunol* 1999; 162:5838-45; PMID:10229818
25. Thompson ED, Enriquez HL, Fu YX, Engelhard VH. Tumor masses support naive T cell infiltration, activation, and differentiation into effectors. *J Exp Med* 2010; 207:1791-804; PMID:20660615; <http://dx.doi.org/10.1084/jem.20092454>
26. Forster R, Braun A, Worbs T. Lymph node homing of T cells and dendritic cells via afferent lymphatics. *Trends Immunol* 2012; 33:271-80; PMID:22459312; <http://dx.doi.org/10.1016/j.it.2012.02.007>
27. Young AJ. The physiology of lymphocyte migration through the single lymph node in vivo. *Semin Immunol* 1999; 11:73-83; PMID:10329494; <http://dx.doi.org/10.1006/smim.1999.0163>
28. Park C, Hwang IY, Sinha RK, Kamenyeva O, Davis MD, Kehrl JH. Lymph node B lymphocyte trafficking is constrained by anatomy and highly dependent upon chemoattractant desensitization. *Blood* 2012; 119:978-89; PMID:22039261; <http://dx.doi.org/10.1182/blood-2011-06-364273>
29. Tomura M, Yoshida N, Tanaka J, Karasawa S, Miwa Y, Miyawaki A, Kanagawa O. Monitoring cellular movement in vivo with photoconvertible fluorescence protein "Kaede" transgenic mice. *Proc Natl Acad Sci U S A* 2008; 105:10871-6; PMID:18663225; <http://dx.doi.org/10.1073/pnas.0802278105>
30. Girard JP, Moussion C, Forster R. HEVs, lymphatics and homeostatic immune cell trafficking in lymph nodes. *Nat Rev Immunol* 2012; 12:762-73; PMID:23018291; <http://dx.doi.org/10.1038/nri3298>
31. Gallatin WM, Weissman IL, Butcher EC. A cell-surface molecule involved in organ-specific homing of lymphocytes. *Nature* 1983; 304:30-4; PMID:6866086; <http://dx.doi.org/10.1038/304030a0>
32. Mackay CR, Marston WL, Dudler L. Naive and memory T cells show distinct pathways of lymphocyte recirculation. *J Exp Med* 1990; 171:801-17; PMID:2307933; <http://dx.doi.org/10.1084/jem.171.3.801>
33. Cose S. T-cell migration: a naive paradigm? *Immunology* 2007; 120:1-7; PMID:17233737; <http://dx.doi.org/10.1111/j.1365-2567.2006.02511.x>
34. Harrell MI, Iritani BM, Ruddell A. Lymph node mapping in the mouse. *J Immunol Methods* 2008; 332:170-4; PMID:18164026; <http://dx.doi.org/10.1016/j.jim.2007.11.012>
35. Debes GF, Arnold CN, Young AJ, Krautwald S, Lipp M, Hay JB, Butcher EC. Chemokine receptor CCR7 required for T lymphocyte exit from peripheral tissues. *Nat Immunol* 2005; 6:889-94; PMID:16116468; <http://dx.doi.org/10.1038/ni1238>
36. Griffith JW, Sokol CL, Luster AD. Chemokines and Chemokine Receptors: Positioning Cells in Host Defense and Immunity. *Annu Rev Immunol* 2014; 32:659-702; PMID:24655300; <http://dx.doi.org/10.1146/annurev-immunol-032713-120145>
37. Bromley SK, Mempel TR, Luster AD. Orchestrating the orchestrators: chemokines in control of T cell traffic. *Nat Immunol* 2008; 9:970-80; PMID:18711434; <http://dx.doi.org/10.1038/ni.f.213>
38. Arai J, Yasukawa M, Yakushijin Y, Miyazaki T, Fujita S. Stromal cells in lymph nodes attract B-lymphoma cells via production of stromal cell-derived factor-1. *Eur J Haematol* 2000; 64:323-32; PMID:10863978; <http://dx.doi.org/10.1034/j.1600-0609.2000.90147.x>
39. Hopken UE, Achtman AH, Kruger K, Lipp M. Distinct and overlapping roles of CXCR5 and CCR7 in B-1 cell homing and early immunity against bacterial pathogens. *J Leukoc Biol* 2004; 76:709-18; PMID:15197239; <http://dx.doi.org/10.1189/jlb.1203643>
40. Cyster JG, Schwab SR. Sphingosine-1-phosphate and lymphocyte egress from lymphoid organs. *Annu Rev Immunol* 2012; 30:69-94; PMID:22149932; <http://dx.doi.org/10.1146/annurev-immunol-020711-075011>
41. Okada T, Ngo VN, Ekland EH, Forster R, Lipp M, Littman DR, Cyster JG. Chemokine requirements for B cell entry to lymph nodes and Peyer's patches. *J Exp Med* 2002; 196:65-75; PMID:12093871; <http://dx.doi.org/10.1084/jem.20020201>
42. Cyster JG. Homing of antibody secreting cells. *Immunol Rev* 2003; 194:48-60; PMID:12846807; <http://dx.doi.org/10.1034/j.1600-065X.2003.00041.x>
43. Beck TC, Gomes AC, Cyster JG, Pereira JP. CXCR4 and a cell-extrinsic mechanism control immature B lymphocyte egress from bone marrow. *J Exp Med* 2014; 211:2567-81; PMID:25403444; <http://dx.doi.org/10.1084/jem.20140457>
44. Reif K, Ekland EH, Ohl L, Nakano H, Lipp M, Forster R, Cyster JG. Balanced responsiveness to chemoattractants from adjacent zones determines B-cell position. *Nature* 2002; 416:94-9; PMID:11882900; <http://dx.doi.org/10.1038/416094a>
45. Forster R, Mattis AE, Kremmer E, Wolf E, Brem G, Lipp M. A putative chemokine receptor, BLR1, directs B cell migration to defined lymphoid organs and specific anatomic compartments of the spleen. *Cell* 1996; 87:1037-47; PMID:8978608; [http://dx.doi.org/10.1016/S0092-8674\(00\)81798-5](http://dx.doi.org/10.1016/S0092-8674(00)81798-5)

46. Pham TH, Okada T, Matloubian M, Lo CG, Cyster JG. S1P1 receptor signaling overrides retention mediated by G  $\alpha$  i-coupled receptors to promote T cell egress. *Immunity* 2008; 28:122-33; PMID:18164221; <http://dx.doi.org/10.1016/j.immuni.2007.11.017>
47. Hopken UE, Foss HD, Meyer D, Hinz M, Leder K, Stein H, Lipp M. Upregulation of the chemokine receptor CCR7 in classical but not in lymphocyte-predominant Hodgkin disease correlates with distinct dissemination of neoplastic cells in lymphoid organs. *Blood* 2002; 99:1109-16; PMID:11830455; <http://dx.doi.org/10.1182/blood.V99.4.1109>
48. Spiegel S, S M. The outs and the ins of sphingosine-1-phosphate in immunity. *Nat Rev Immunol* 2011; 11:403-15; PMID:21546914; <http://dx.doi.org/10.1038/nri2974>
49. Garris CS, Blaho VA, Hla T, Han MH. Sphingosine-1-phosphate receptor 1 signalling in T cells: trafficking and beyond. *Immunology* 2014; 142:347-53; PMID:24597601; <http://dx.doi.org/10.1111/imm.12272>
50. Thangada S, Khanna KM, Blaho VA, Oo ML, Im DS, Guo C, L L, Hla T. Cell-surface residence of sphingosine 1-phosphate receptor 1 on lymphocytes determines lymphocyte egress kinetics. *J Exp Med* 2010; 207:1475-83; PMID:20584883; <http://dx.doi.org/10.1084/jem.20091343>
51. Bankovich AJ, Shiow LR, Cyster JG. CD69 suppresses sphingosine 1-phosphate receptor-1 (S1P1) function through interaction with membrane helix 4. *J Biol Chem* 2010; 285:22328-37; PMID:20463015; <http://dx.doi.org/10.1074/jbc.M110.123299>
52. Marzio R, Mauel J, Betz-Corradin S. CD69 and regulation of the immune function. *Immunopharmacol Immunotoxicol* 1999; 21:565-82; PMID:10466080; <http://dx.doi.org/10.3109/08923979909007126>
53. Sensken SC, Nagarajan M, Bode C, Graler MH. Local inactivation of sphingosine 1-phosphate in lymph nodes induces lymphopenia. *J Immunol* 2011; 186:3432-40; PMID:21289303; <http://dx.doi.org/10.4049/jimmunol.1002169>
54. Chiba K, Matsuyuki H, Maeda Y, Sugahara K. Role of sphingosine 1-phosphate receptor type 1 in lymphocyte egress from secondary lymphoid tissues and thymus. *Cell Mol Immunol* 2006; 3:11-9; PMID:16549044
55. Schulz O, Ugur M, Friedrichsen M, Radulovic K, Niess JH, Jalkanen S, Krueger A, Pabst O. Hypertrophy of infected Peyer's patches arises from global, interferon-receptor, and CD69-independent shutdown of lymphocyte egress. *Mucosal Immunol* 2014; 7:892-904; PMID:24345804; <http://dx.doi.org/10.1038/mi.2013.105>
56. Mudd JC, Murphy P, Manion M, Debernardo R, Hardacre J, Ammori J, Hardy GA, Harding CV, Mahabaleshwar GH, Jain MK et al. Impaired T-cell responses to sphingosine-1-phosphate in HIV-1 infected lymph nodes. *Blood* 2013; 121:2914-22; PMID:23422746; <http://dx.doi.org/10.1182/blood-2012-07-445783>
57. Pappu R, Schwab SR, Cornelissen I, Pereira JP, Regard JB, Xu Y, Camerer E, Zheng YW, Huang Y, Cyster JG et al. Promotion of lymphocyte egress into blood and lymph by distinct sources of sphingosine-1-phosphate. *Science* 2007; 316:295-8; PMID:17363629; <http://dx.doi.org/10.1126/science.1139221>
58. Pham TH, Baluk P, Xu Y, Grigorova I, Bankovich AJ, Pappu R, Coughlin SR, McDonald DM, Schwab SR, Cyster JG. Lymphatic endothelial cell sphingosine kinase activity is required for lymphocyte egress and lymphatic patterning. *J Exp Med* 2009; 207:17-27; PMID:20026661; <http://dx.doi.org/10.1084/jem.20091619>
59. Takabe K, Spiegel S. Export of sphingosine-1-phosphate and cancer progression. *J Lipid Res* 2014; 55:1839-46; PMID:24474820; <http://dx.doi.org/10.1194/jlr.R046656>
60. Mackay LK, Braun A, Macleod BL, Collins N, Tebartz C, Bedoui S, Carbone FR, Gebhardt T. Cutting edge: CD69 interference with sphingosine-1-phosphate receptor function regulates peripheral T cell retention. *J Immunol* 2015; 194:2059-63; PMID:25624457; <http://dx.doi.org/10.4049/jimmunol.1402256>
61. Overwijk WW, Restifo NP. B16 as a mouse model for human melanoma. *Current Protocols in Immunology*. Philadelphia PA: John Wiley and Sons, Inc, 2000:20.1-9.
62. Hargadon KM, Brinkman CC, Sheasley-O'neill S L, Nichols LA, Bullock TN, Engelhard VH. Incomplete differentiation of antigen-specific CD8 T cells in tumor-draining lymph nodes. *J Immunol* 2006; 177:6081-90; PMID:17056534; <http://dx.doi.org/10.4049/jimmunol.177.9.6081>
63. Aoki M, Aoki H, Ramanathan R, Hait NC, Takabe K. Sphingosine-1-Phosphate Signaling in Immune Cells and Inflammation: Roles and Therapeutic Potential. *Mediators Inflamm* 2016; 2016:8606878; PMID:26966342; <http://dx.doi.org/10.1155/2016/8606878>
64. Patmanathan SN, Yap LF, Murray PG, Paterson IC. The antineoplastic properties of FTY720: evidence for the repurposing of fingolimod. *J Cell Mol Med* 2015; 19:2329-40; PMID:26171944; <http://dx.doi.org/10.1111/jcmm.12635>
65. Zhang L, Wang X, Bullock AJ, Callea M, Shah H, Song J, Moreno K, Visentin B, Deutschman D, Alsop DC et al. Anti-S1P Antibody as a Novel Therapeutic Strategy for VEGFR TKI-Resistant Renal Cancer. *Clin Cancer Res* 2015; 21:1925-34; PMID:25589614; <http://dx.doi.org/10.1158/1078-0432.CCR-14-2031>
66. Anderson ND, Anderson AO, Wylie RG. Microvascular changes in lymph nodes draining skin allografts. *Am J Pathol* 1975; 81:131-60; PMID:1101703
67. Eidsmo L, Stock AT, Heath WR, Bedoui S, Carbone FR. Reactive murine lymph nodes uniquely permit parenchymal access for T cells that enter via the afferent lymphatics. *J Pathol* 2012; 226:806-13; PMID:22170282; <http://dx.doi.org/10.1002/path.3975>
68. Brown MN, Fintushel SR, Lee MH, Jennrich S, Geherin SA, Hay JB, Butcher EC, Debes GF. Chemoattractant receptors and lymphocyte egress from extralymphoid tissue: changing requirements during the course of inflammation. *J Immunol* 2010; 185:4873-82; PMID:20833836; <http://dx.doi.org/10.4049/jimmunol.1000676>
69. Hall JG, Morris B. The Origin of the Cells in the Efferent Lymph from a Single Lymph Node. *J Exp Med* 1965; 121:901-10; PMID:14319406; <http://dx.doi.org/10.1084/jem.121.6.901>
70. Gomez D, Diehl MC, Crosby EJ, Weinkopff T, Debes GF. Effector T Cell Egress via Afferent Lymph Modulates Local Tissue Inflammation. *J Immunol* 2015; 195:3531-6; PMID:26355150; <http://dx.doi.org/10.4049/jimmunol.1500626>
71. Geherin SA, Wilson RP, Jennrich S, Debes GF. CXCR4 is dispensable for T cell egress from chronically inflamed skin via the afferent lymph. *PLoS One* 2014; 9:e95626; PMID:24752354; <http://dx.doi.org/10.1371/journal.pone.0095626>
72. Fox BA, Schendel DJ, Butterfield LH, Aamdal S, Allison JP, Ascierto PA, Atkins MB, Bartunkova J, Bergmann L, Berinstein N et al. Defining the critical hurdles in cancer immunotherapy. *J Transl Med* 2011; 9:214; PMID:22168571; <http://dx.doi.org/10.1186/1479-5876-9-214>
73. Inman CF, Murray TZ, Bailey M, Cose S. Most B cells in non-lymphoid tissues are naive. *Immunol Cell Biol* 2012; 90:235-42; PMID:21556017; <http://dx.doi.org/10.1038/icb.2011.35>
74. Affara N, Ruffell B, Medler T, Gunderson A, Johansson M, Bornstein S, Bergsland E, Steinhoff M, Li Y, Gong W et al. B cells regulate macrophage phenotype and response to chemotherapy in squamous carcinomas. *Cancer Cell* 2014; 25:809-21; PMID:24909985; <http://dx.doi.org/10.1016/j.ccr.2014.04.026>
75. Gunderson AJ, Kaneda MM, Tsujikawa T, Nguyen AV, Affara NI, Ruffell B, Gorjestani S, Liudahl SM, Truitt M, Olson P et al. Bruton's Tyrosine Kinase (BTK)-dependent immune cell crosstalk drives pancreas cancer. *Cancer Discov* 2015; 6:270-285; PMID:26715645; <http://dx.doi.org/10.1158/2159-8290.CD-15-0827>
76. Zhang Y, Gallastegui N, Rosenblatt JD. Regulatory B cells in anti-tumor immunity. *Int Immunol* 2015; 27:521-30; PMID:25999597; <http://dx.doi.org/10.1093/intimm/dxv034>
77. Nakai A, Hayano Y, Furuta F, Noda M, Suzuki K. Control of lymphocyte egress from lymph nodes through beta2-adrenergic receptors. *J Exp Med* 2014; 211:2583-98; PMID:25422496; <http://dx.doi.org/10.1084/jem.20141132>
78. Card CM, Yu SS, Swartz MA. Emerging roles of lymphatic endothelium in regulating adaptive immunity. *J Clin Invest* 2014; 124:943-52; PMID:24590280; <http://dx.doi.org/10.1172/JCI73316>
79. Rouhani SJ, Eccles JD, Tewalt EF, Engelhard VH. Regulation of T-cell Tolerance by Lymphatic Endothelial Cells. *J Clin Cell Immunol* 2014; 5:242-250; PMID:25580369; <http://dx.doi.org/10.4172/2155-9899.1000242>
80. Visentin B, Vekich JA, Sibbald BJ, Cavalli AL, Moreno KM, Matteo RG, Garland WA, Lu Y, Yu S, Hall HS et al. Validation of an anti-sphingosine-1-phosphate antibody as a potential therapeutic in reducing growth, invasion, and angiogenesis in multiple tumor lineages. *Cancer Cell* 2006; 9:225-38; PMID:16530706; <http://dx.doi.org/10.1016/j.ccr.2006.02.023>